

UNCLASSIFIED

AD 257 484

*Reproduced  
by the*

ARMED SERVICES TECHNICAL INFORMATION AGENCY  
ARLINGTON HALL STATION  
ARLINGTON 12, VIRGINIA



20050204/58

UNCLASSIFIED

Best Available Copy

NOTICE: When government or other drawings, specifications or other data are used for any purpose other than in connection with a definitely related government procurement operation, the U. S. Government thereby incurs no responsibility, nor any obligation whatsoever; and the fact that the Government may have formulated, furnished, or in any way supplied the said drawings, specifications, or other data is not to be regarded by implication or otherwise as in any manner licensing the holder or any other person or corporation, or conveying any rights or permission to manufacture, use or sell any patented invention that may in any way be related thereto.

2025-02-01

DocId: 34411111

**Summary Technical Report**

**On**

**An Investigation of Methods for Determining  
the Crack-Propagation Resistance  
of High-Strength Alloys**

**By**

**J. D. Morrison  
J. R. Kattus**

**March 7, 1961**

**Prepared under Bureau of Naval Weapons  
Contract NOas 60-6040c**

**14 October 1959 through 14 January 1961**

**Southern Research Institute  
Birmingham, Alabama**

## FOREWORD

This is the summary technical report covering the work done during the period from October 14, 1959, through January 13, 1961, on Contract NOas 60-6040c for the Bureau of Naval Weapons. The program was monitored by Mr. G. M. Yoder, RRMA-212, Head, Ferrous Alloys Section, Bureau of Naval Weapons.

The following personnel at Southern Research Institute made significant contributions to the project:

1. F. R. O'Brien, Assistant Director
2. J. B. Preston, Senior Engineer
3. H. L. Lessley, Associate Engineer
4. O. V. Rogers, Associate Engineer
5. M. A. Campbell, Assistant Metallurgist
6. W. L. Rogers, Research Technician
7. D. E. Rice, Research Technician

The guidance and cooperation of Mr. T. F. Kearns and Mr. G. M. Yoder, of the Bureau of Naval Weapons, and Mr. J. E. Srawley, of the Naval Research Laboratory, are gratefully acknowledged. The cooperation of personnel of the Kidde Aero-Space Division, Walter Kidde and Company, Belleville, New Jersey, is acknowledged with thanks.

### ABSTRACT

The purpose of the investigation described in this report was several-fold, covering mainly the following points: 1) to devise a simple crack-propagation specimen for evaluating high-strength sheet materials; 2) to determine the crack-propagation characteristics of several high-strength sheet materials; 3) to determine the effects of several experimental variables on the crack-propagation characteristics of some of these materials; and 4) to determine the validity of the crack-propagation specimen for predicting the biaxial strength of the high-strength sheet materials. A sheet specimen called the "shear-cracked" specimen was used extensively in the investigation. This specimen, which contains a central transverse crack or notch produced by means of a simple punch-and-die fixture, can be produced very rapidly and economically.

It was established that the crack-propagation properties obtained with the shear-cracked specimen were very similar to those obtained with fatigue-cracked specimens of the quench-hardenable and age-hardenable materials. A comparison of the crack-propagation properties obtained with sheet specimens and the burst strengths of model pressure vessels of two steels (AISI 4130 and AISI 4340) indicated that the sheet-type crack-propagation specimen may be useful in predicting the biaxial strength of materials heat treated to very high strength levels (in excess of about 250,000 psi). At lower nominal strength levels, the crack-propagation specimen is apparently too "severe" a criterion of the biaxial strength behavior of sheet materials.

## TABLE OF CONTENTS

<u>Section</u>	<u>Page</u>
I INTRODUCTION . . . . .	1
II BASIS FOR EXPERIMENTAL APPROACH . . . . .	2
III EXPERIMENTAL PROGRAM . . . . .	4
A. Materials Evaluated . . . . .	4
B. Specimens . . . . .	6
C. Equipment and Procedure . . . . .	9
D. Electrical Measurement of Slow-Crack Extension . . . . .	12
IV EXPERIMENTAL RESULTS . . . . .	13
A. Evaluation of Crack-Propagation Character- istics of Sheet Materials . . . . .	13
1. Low-Alloy Steels and Stainless Steels . .	13
2. Aluminum Alloys . . . . .	29
B. Evaluation of Model Pressure Vessels . . . . .	35
C. Effects of experimental Variables on Crack- Propagation Characteristics of Sheet Materials . . . . .	44
1. Effect of Loading Rate on Crack- Propagation Characteristics . . . . .	45
2. Effect of Tempering Temperature on Transition Temperature of AISI 4130 Steel . . . . .	49
3. Effect of Sheet Thickness on Transi- tion Temperature of AISI 4130 Steel . . .	51
D. Comparison of Crack-Propagation Data Obtained with Different Types of Specimens .	51
V CONCLUSIONS . . . . .	58
BIBLIOGRAPHY . . . . .	60
APPENDIX A . . . . .	61
APPENDIX B . . . . .	108

### LIST OF ILLUSTRATIONS

<u>Figure No.</u>		<u>Page</u>
1	Sheet tensile specimen . . . . .	7
2	Typical shear-cracked specimen . . . . .	8
3	Longitudinal section of model pressure vessel used for determining burst properties of AISI 4130 steel. Vessels fabricated from AISI 4340 steel were similar but were 3.52 in. in diameter . . . . .	10
4	Effect of temperature on the standard-tensile properties and fracture properties of heat-treated longitudinal specimens of AMS 6434 steel sheet. . . . .	16
5	Appearance of fracture surfaces of shear-cracked AMS 6434 steel sheet loaded to failure at temperatures from -200° F to 600° F. . . . .	17
6	Effect of temperature on the standard-tensile properties and fracture properties of heat-treated longitudinal specimens of 300 Ni steel sheet . . . . .	18
7	Effect of temperature on the standard-tensile properties and fracture properties of longitudinal specimens of full-hard Type 301 stainless steel sheet . . . . .	19
8	Effect of temperature on the standard-tensile properties and fracture properties of heat-treated, longitudinal specimens of AISI 4130 steel sheet . . . . .	20
9	Effect of temperature on the standard-tensile properties and fracture properties of heat-treated, longitudinal specimens of AM 350 sheet, loaded to fracture in 2 min . . . . .	21
10	Effect of temperature on the standard-tensile properties and fracture properties of heat-treated longitudinal specimens of 17-7 PH sheet, loaded to fracture at a slow rate. . . . .	22

LIST OF ILLUSTRATIONS (Continued)

<u>Figure No</u>		<u>Page</u>
11	Effect of temperature on the standard tensile properties and fracture properties of AISI 4130 steel sheet specimens . . . . .	23
12	Effect of temperature on the fracture toughness and fracture appearance of shear-cracked specimens of AISI 4130 steel sheet . . . . .	24
13	Effect of temperature on the standard tensile properties and fracture properties of AISI 4130 steel sheet specimens . . . . .	25
14	Effect of temperature on the standard tensile strength properties and fracture strength properties (obtained with two types of shear-cracked specimens) of quenched and tempered AISI 4340 steel sheet . . . . .	26
15	Effect of temperature on the standard tensile properties and the net fracture strength of aged Inconel X sheet . . . . .	27
16	Effect of temperature on the net fracture stress and fracture appearance of shear-cracked AISI 4340 sheet specimens. Specimens were 1.87 in. over-all width and 0.120 in. thick . . . . .	28
17	Effect of holding time after rapid heating on the tensile properties and fracture strength of 7075-T6 aluminum sheet loaded rapidly to failure at different temperatures . . . . .	31
18	Effect of holding time after rapid heating on the tensile properties and fracture properties of 7079-T6 aluminum sheet loaded rapidly to failure at different temperatures . . . . .	32
19	Effect of holding time after rapid heating on the tensile properties and fracture strength of 2024-T86 aluminum sheet loaded rapidly to failure at different temperatures . . . . .	33



LIST OF ILLUSTRATIONS (Continued)

<u>Figure No</u>		<u>Page</u>
20	Effect of holding time after rapid heating on the tensile properties and fracture strength of X2020-T6 aluminum sheet loaded rapidly to failure at different temperatures . . . . .	34
21	Effect of temperature on the fracture properties of AISI 4130 steel vessels and on the standard tensile properties of AISI 4130 steel sheet specimens . . . . .	36
22	Typical model vessels of AISI 4130 steel, heat treated to 200,000 psi strength level, fractured at temperatures from -160° F to 365° F . . . . .	37
23	Effect of temperature on the burst properties of AISI 4130 steel vessels and on the standard tensile properties and fracture properties of AISI 4130 steel sheet specimens . . . . .	38
24	Effect of temperature on the burst properties of AISI 4340 steel vessels and the fracture properties of shear-cracked specimens of AISI 4340 steel sheet . . . . .	39
25	Typical vessels of AISI 4340 steel (240,000 - 262,000 psi nominal strength level) fractured at 75° F . . . . .	41
26	Typical vessels of AISI 4340 steel (240,000 - 262,000 psi nominal strength level) fractured at -20° F . . . . .	42
27	Typical vessels of AISI 4340 steel (240,000 - 262,000 psi nominal strength level) fractured at -105° F . . . . .	43
28	Effect of loading rate on the fracture properties of longitudinal, shear-cracked, AM 350 sheet at various temperatures . . . . .	46
29	Effect of loading rate on the fracture properties of longitudinal, fatigue-cracked AM 350 sheet at various temperatures . . . . .	47

LIST OF ILLUSTRATIONS (Continued)

<u>Figure No.</u>		<u>Page</u>
30	Effect of loading rate on fracture-properties, at various temperatures, of heat-treated longitudinal fatigue-cracked specimens of 17-7 PH sheet. . . . .	48
31	Effect of tempering temperature on the crack-propagation properties of AISI 4130 steel sheet (0.103 in. thick) at various temperatures. . . . .	50
32	Effect of sheet thickness on the crack-propagation properties of AISI 4130 steel (at the 240,000 psi strength level) at various temperatures. . . . .	51
33	Effect of temperature on the standard tensile properties and fracture properties of heat-treated, longitudinal specimens of AM 350 sheet, loaded to fracture in 2 min. . . . .	54
34	Effect of temperature on the standard tensile properties and fracture properties of heat-treated longitudinal specimens of 17-7 PH sheet, loaded to fracture at a slow rate. . . . .	54
35	Comparison of fracture-strength data obtained with shear-cracked and fatigue-cracked specimens of 7075-T6 aluminum sheet loaded rapidly to failure at various temperatures after holding for 1800 sec at temperature. . . . .	55
36	Comparison of fracture-strength data obtained with shear-cracked and fatigue-cracked specimens of 7079-T6 aluminum sheet loaded rapidly to failure at various temperatures after holding for 1800 sec at temperature. . . . .	55
37	Comparison of fracture-strength data obtained with shear-cracked and fatigue-cracked specimens of 2024-T86 aluminum alloy sheet loaded rapidly to failure at various temperatures after holding for 1800 sec at temperature. . . . .	56

LIST OF ILLUSTRATIONS (Continued)

<u>Figure No.</u>		<u>Page</u>
38	Comparison of fracture strength data obtained with shear-cracked and fatigue-cracked specimens of X2020-T6 aluminum sheet loaded rapidly to failure at various temperatures after holding for 1800 sec at temperature . . . . .	56
39	Comparison of fracture properties at various temperatures obtained with two different types of crack-propagation specimens of AISI 4130 steel . . . . .	57

## LIST OF TABLES

<u>Table No.</u>		<u>Page</u>
1	Sheet Materials Evaluated . . . . .	4
2	Model Pressure Vessel Materials and Conditions . . . . .	6
3	Tensile Properties of Heat-Treated AMS 6434 Steel Sheet at Different Temperatures, and at a Nominal Strain Rate of 0.0001 in. /in. /sec. . . . .	62
4	Fracture Strength of Cracked Heat-Treated AMS 6434 Steel Sheet at Different Temperatures . . . . .	63
5	Tensile Properties of Heat-Treated 300 M Steel Sheet at Different Temperatures, and at a Nominal Strain Rate of 0.0001 in. /in. /sec . . . . .	64
6	Fracture Strength of Cracked Heat-Treated 300 M Steel Sheet at Different Temperatures . . . . .	65
7	Fracture Strength of Cracked Full-Hard Type 301 Stainless Steel Sheet at Different Temperatures . . . . .	66
8	Tensile Properties of Heat-Treated AISI 4130 Steel Sheet at Different Temperatures, and at a Nominal Strain Rate of 0.0001 in. /in. /sec . . . . .	67
9	Fracture Strength of Cracked Heat-Treated AISI 4130 Steel at Different Temperatures . . . . .	68
10	Tensile Properties of Heat-Treated AM 350 Stainless Steel Sheet at Different Temperatures and at a Nominal Strain Rate of 0.0001 in. /in. /sec . . . . .	69
11	Fracture Strength of Shear-Cracked Heat-Treated AM 350 Sheet at Different Temperatures . . . . .	70
12	Tensile Properties of Heat-Treated 17-7 PH Stainless Steel Sheet at Different Temperatures, and at a Nominal Strain Rate of 0.0001 in. /in. /sec . . . . .	71

# LIST OF TABLES (Continued)

<u>Table No.</u>		<u>Page</u>
13	Fracture Strength of Shear-Cracked 17-7 PH Stainless Steel Sheet at Different Temperatures . . . . .	72
14	Tensile Properties of Heat-Treated AISI 4130 Steel Sheet at Different Temperatures and at a Nominal Strain Rate of 0.0001 in. /in. /sec . . . . .	74
15	Fracture Strength of Shear-Cracked Heat-Treated AISI 4130 Steel Sheet at Different Temperatures . . . . .	76
16	Tensile Properties of Heat-Treated AISI 4130 Steel Sheet at Different Temperatures, and at a Nominal Strain Rate of 0.0001 in. /in. /sec . . . . .	78
17	Fracture Strength of Shear-Cracked AISI 4130 Steel Sheet at Different Temperatures . . . . .	79
18	Tensile Properties of Heat-Treated AISI 4340 Steel Sheet at Different Temperatures and at a Nominal Strain Rate of 0.0001 in. /in. /sec . . . . .	80
19	Fracture Strength of Shear-Cracked AISI 4340 Steel Sheet at Different Temperatures . . . . .	19
19A	Fracture Strength of Shear-Cracked AISI 4340 Steel Sheet at Different Temperatures . . . . .	82
20	Tensile Properties of Aged Inconel X Sheet at Different Temperatures and at a Nominal Strain Rate of 0.0001 in. /in. /sec . . . . .	83
21	Fracture Strength of Shear-Cracked Inconel X Sheet at Different Temperatures . . . . .	84
22	Fracture Strength of Shear-Cracked Heat Treated AISI 4340 Steel Sheet at Different Temperatures . . . . .	86
23	Tensile Properties of 7075-T6 Aluminum Alloy Sheet at Different Temperatures, Holding Times, and at a Nominal Strain Rate of 0.1 in. /in. /sec . . . . .	87

# LIST OF TABLES (Continued)

<u>Table No.</u>		<u>Page</u>
24	Fracture Strength of Shear-Cracked 7075-T6 Aluminum Alloy Sheet at Different Temperatures and Holding Times . . . . .	88
25	Tensile Properties of 7073-16 Aluminum Alloy Sheet at Different Temperatures, Holding Times, and at a Nominal Strain Rate of 0.1 in. /in. /sec . . . . .	89
26	Fracture Strength of Shear-Cracked 7079-T6 Aluminum Alloy Sheet at Different Temperatures and Holding Times . . . . .	90
27	Tensile Properties of 2024-T86 Aluminum Alloy Sheet at Different Temperatures, Holding Times, and at a Nominal Strain Rate of 0.1 in. /in. /sec . . . . .	91
28	Fracture Strength of Shear-Cracked 2024-T86 Aluminum Alloy Sheet at Different Temperatures and Holding Times . . . . .	92
29	Tensile Properties of X2020-T6 Aluminum Alloy Sheet at Different Temperatures, Holding Times, and at a Nominal Strain Rate of 0.1 in. /in. /sec . . . . .	93
30	Fracture Strength of Shear-Cracked X2020-T6 Aluminum Alloy Sheet at Different Temperatures and Holding Times . . . . .	94
31	Burst Properties of AISI 4130 Model Vessels Fractured at Different Temperatures . . . . .	95
32	Burst Properties of AISI 4130 Model Vessels Fractured at Different Temperatures . . . . .	96
33	Burst Properties of AISI 4340 Model Vessels Fractured at Different Temperatures . . . . .	97
34	Fracture Strength of Shear-Cracked AM 350 Stainless Steel Sheet at Different Temperatures . . . . .	98

LIST OF TABLES (Continued)

<u>Table No.</u>		<u>Page</u>
35	Fracture Strength of Fatigue-Cracked AM 350 Stainless Steel Sheet at Different Temperatures . . . . .	99
35A	Fracture Strength of Fatigue-Cracked Heat-Treated AM 350 Sheet at Different Temperatures . . . . .	100
36	Fracture Strength of Fatigue-Cracked 17-7 PH Stainless Steel Sheet at Different Temperatures . . . . .	101
37	Fracture Strength of Fatigue-Cracked 17-7 PH Stainless Steel Sheet at Different Temperatures . . . . .	102
38	Fracture Strength of Fatigue-Cracked 7075-T6 Aluminum Alloy Sheet at Different Temperatures . . . . .	103
39	Fracture Strength of Fatigue-Cracked 7079-T6 Aluminum Alloy Sheet at Different Temperatures . . . . .	104
40	Fracture Strength of Fatigue-Cracked 2024-T86 Aluminum Alloy Sheet at Different Temperatures . . . . .	105
41	Fracture Strength of Fatigue-Cracked X2020-T6 Aluminum Alloy Sheet at Different Temperatures . . . . .	106
42	Fracture Strength of Fatigue-Cracked AISI 4130 Steel Sheet at Different Temperatures . . . . .	107

An Investigation of Methods for Determining  
the Crack-Propagation Resistance  
of High-Strength Alloys

I. INTRODUCTION

The general purposes of this program were to establish a valid and simple laboratory method for assessing the resistance to crack propagation of high-strength structural materials and to use this method to evaluate the crack-propagation resistance of a number of alloys under various conditions of temperature and loading. Such information is needed in the selection of materials for highly-stressed structures such as high-speed aircraft and rocket-motor casings. The need for a minimum-weight structure in these applications has dictated the use of ultra-high strength sheet materials that normally have inherently low resistance to crack propagation. In addition, many of the service conditions to which these structures may be exposed, such as low temperatures and high rates of stressing, impose further embrittling tendencies. As a result of these over-all "embrittling effects," failures of these "high-strength" materials have occurred at applied stresses well below their yield strengths.

The scope of the program embraces the points listed below in the form of brief statements, in the order of their presentation in the report. These aims are:

1. To furnish crack-propagation data on various high-strength alloys in a useful range of temperatures.
2. To attempt to correlate crack-propagation data obtained with small sheet specimens with burst properties of model pressure vessels of the same material.
3. To investigate the effects of the following experimental variables on crack-propagation properties:
  - (a) loading rate
  - (b) tempering temperature of steels
  - (c) sheet thickness
4. To compare different types of crack-propagation specimens for similarities and differences in the "properties" they indicate for a given material.



The order of presentation of these points is not meant to imply their relative importance; rather, it represents a rational method of presentation for the best utilization of the experimental data.

### 1. BASIS FOR EXPERIMENTAL APPROACH

The ASTM Committee on Fracture Testing of High-Strength Sheet Materials has recently published (1)<sup>1</sup> recommended techniques for determining crack-propagation characteristics. In these articles, the Committee recommended the use of two sorts of tensile specimens, the specimens containing either sharp-edge notches or central crack-like defects. In the investigation described in this report, a specimen design of the latter type was used extensively. This design is referred to as the "shear-cracked specimen" (Figure 2) and is essentially a modification of the central fatigue-cracked specimen used by Srawley and Beachem (2). The shear-cracked specimen has the advantage of being easily and economically prepared, with quite reproducible crack dimensions.

Three general types of criteria for crack-propagation resistance are often obtained with the notched or cracked sheet specimens. These types are: 1) notch strength or, equivalently, net fracture stress, these values being "nominal strengths" obtained by dividing the ultimate load by the original net supporting area; 2) "percent shear" in the fracture, which is a quantitative estimate of that percentage of the fracture surface in which separation by shear occurred; and 3) the "fracture-toughness" parameters— $G_C$  and  $K_{IC}$ —which are more fundamental material properties that may be determined with the aid of the Griffith-Irwin fracture-mechanics theory. These terms are defined in reference (1). The larger the values of  $G_C$  or  $K_{IC}$ , the greater is the resistance of the material to crack propagation.

These three criteria may be used to define brittle-to-ductile transition temperatures in the following ways. 1) The net-fracture-stress transition temperature is often defined as the lowest temperature at which the net fracture stress is equal to the yield stress. For some materials, it is more convenient to define this transition temperature as the temperature below which there is a sharp reduction in net fracture stress. 2) The "full-shear" transition temperature, which is based upon the fracture appearance, is the lowest temperature at which failure occurs with 100% shear. 3) A transition temperature may be

<sup>1</sup> Numbers in parentheses refer to the bibliography.

defined in terms of the critical fracture-toughness parameters— $K_{IC}$ , the stress-intensity factor, and  $G_{IC}$ , the crack-extension force—as the temperature below which there is a sharp reduction in fracture toughness.

The specimen-design recommendations of the ASTM Committee for fracture-toughness evaluations have been given in detail in the ASTM Bulletin (1); these requirements are briefly summarized as follows:

1. The specimen width-to-thickness ratio should be in the range from 16-to-1 to 45-to-1.
2. The length of the specimen should be such that the loading-pin holes will be at least 2.5 specimen-widths apart.
3. The initial crack-length to specimen-width ratio should be from about 0.3 to 0.4, for center-cracked specimens. For edge-notched specimens, the width of the unnotched section should be 70% of the overall specimen width.

If these requirements are met with the sheet specimen, it is then possible to calculate the fracture-toughness parameter,  $K_{IC}$ , when the ultimate load and the critical crack-length are known. The critical crack-length may be established by marking the extent of slow crack-extension by means of a dye, such as India ink, or by other means. Alternatively, an estimate of critical crack length may be calculated from the length of the starting crack and the percent shear in the fracture surface (1). The fracture-toughness parameter calculated from these latter values is referred to as  $K_{IC}$ .

From the calculated  $K_{IC}$  values, it is possible to estimate the maximum flaw size that can be allowed in a structure fabricated from a given sheet material and to estimate the yield-strength level that will attain the best "balance" between yield strength and fracture toughness, so that the probability of brittle fracture at stresses below the yield strength is minimized.

### III. EXPERIMENTAL PROGRAM

In the evaluations of the sheet materials, it was the general practice to obtain the standard tensile properties and the crack-propagation properties of each material over a range of temperatures that would cover the expected service temperatures of the material. A slow rate of loading was usually employed, such that the specimens generally fractured in from 2 to 4 minutes. In one phase of the evaluation program, the fracture properties of four aluminum alloys were obtained under very specialized conditions of heating and loading that simulated certain service conditions to which aircraft structures, fabricated from these alloys, may be exposed. The exact experimental conditions used for each material and the details of the program to correlate fracture toughness of sheet materials with "service performance" of model pressure vessels will be given in subsequent sections.

#### A. Materials Evaluated

In Table 1, a list is given of all of the sheet materials that were evaluated, with the sheet thicknesses and the heat treatments used.

Table 1

#### Sheet Materials Evaluated

<u>Material</u>	<u>Sheet Thickness, in.</u>	<u>Condition</u>
AMS 6434 (low-alloy steel)	0.064	Oil-quenched from 1620° F; tempered at 400° F for 2 hr
300M (low-alloy steel)	0.080	Oil-quenched from 1600° F; double tempered at 600° F for 3 hr each cycle
Type 301 (austenitic stainless- steel)	0.046	50% cold reduced
AISI 4130 (low-alloy steel)	0.042	Oil-quenched from 1570° F; tempered at 400° F for 2 hr

Table 1 (Continued)

Sheet Materials Evaluated

<u>Material</u>	<u>Sheet Thickness, in</u>	<u>Condition</u>
AM 350 (semi-austenitic stainless steel)	0.040	Water-quenched from 1725° F; refrigerated at -105° F for 3 hr; aged at 850° F for 3 hr.
17-7 PH (precipitation- hardening stainless steel)	0.040	Air cooled from 1400° F; held at 50° F for 1 hr; aged at 1050° F for 1 1/2 hr
AISI 4130 (low-alloy steel)	0.100	Oil-quenched from 1700° F; tempered at 825° F for 1 hr
AISI 4130 (low-alloy steel)	0.100	Oil-quenched from 1700° F; tempered at 400° F for 2 hr
AISI 4340 (low-alloy steel)	0.064	Oil-quenched from 1600° F; double tempered at 400° F for 2 hr each cycle
Inconel-X (nickel-base alloy)	0.064	Aged at 1300° F for 24 hr
AISI 4340 (low-alloy steel)	0.120	Oil-quenched from 1600° F; tempered at 425° F for 2 hr
7075 Aluminum	0.064	T-6
7079 Aluminum	0.064	T-6
2024 Aluminum	0.064	T-86
X 2020 Aluminum	0.064	T-6

Seamless model pressure vessels of AISI 4130 and AISI 4340 steel were obtained from the fabricator, the Kidde Aero-Space Division. The heat treatments used to obtain given nominal strength levels in these vessels are shown in Table 2.

Table 2  
Model Pressure Vessel Materials and Conditions

Material	Nominal Strength Level	Condition
AISI 4130 (low-alloy steel)	200,000 psi	Oil-quenched from 1700° F; tempered at 825° F for 1 hr
AISI 4130 (low-alloy steel)	240,000 psi	Oil-quenched from 1700° F; tempered at 400° F for 1 hr
AISI 4340 (low-alloy steel)	240,000 - 262,000 psi	Oil-quenched from 1600° F; tempered at 425° F for 2 hr

#### B. Specimens

Standard tensile specimens prepared from each of the sheet materials had gage-sections 2 in. long by 3/8 in. wide. A typical tensile specimen is shown in Figure 1.

The "lugs" at the specimen gage-points were used to actuate a special "clip-on" extensometer that can be used to measure strain over a wide range of specimen temperatures.

The shear-cracked specimens, used to obtain the crack-propagation data, were prepared with a special punch-and-die fixture that makes a transverse slit of the desired length through the thickness of the specimen. A typical shear-cracked specimen is shown in Figure 2. Four punch-and-die fixtures were available for making shear-cracks of the following lengths: 0.20 in., 0.35 in., 0.58 in., and about 1.05 in. These fixtures can be used on sheet thicknesses up to 1/8 in. This variety of obtainable shear-crack lengths is suitable for specimen widths up to 3 in. Generally, two widths of crack-propagation specimens were used in this work. For sheet thicknesses from 0.040 in. to 0.060 in., specimens 1.5 in. wide were used, with a shear-crack length of 0.58

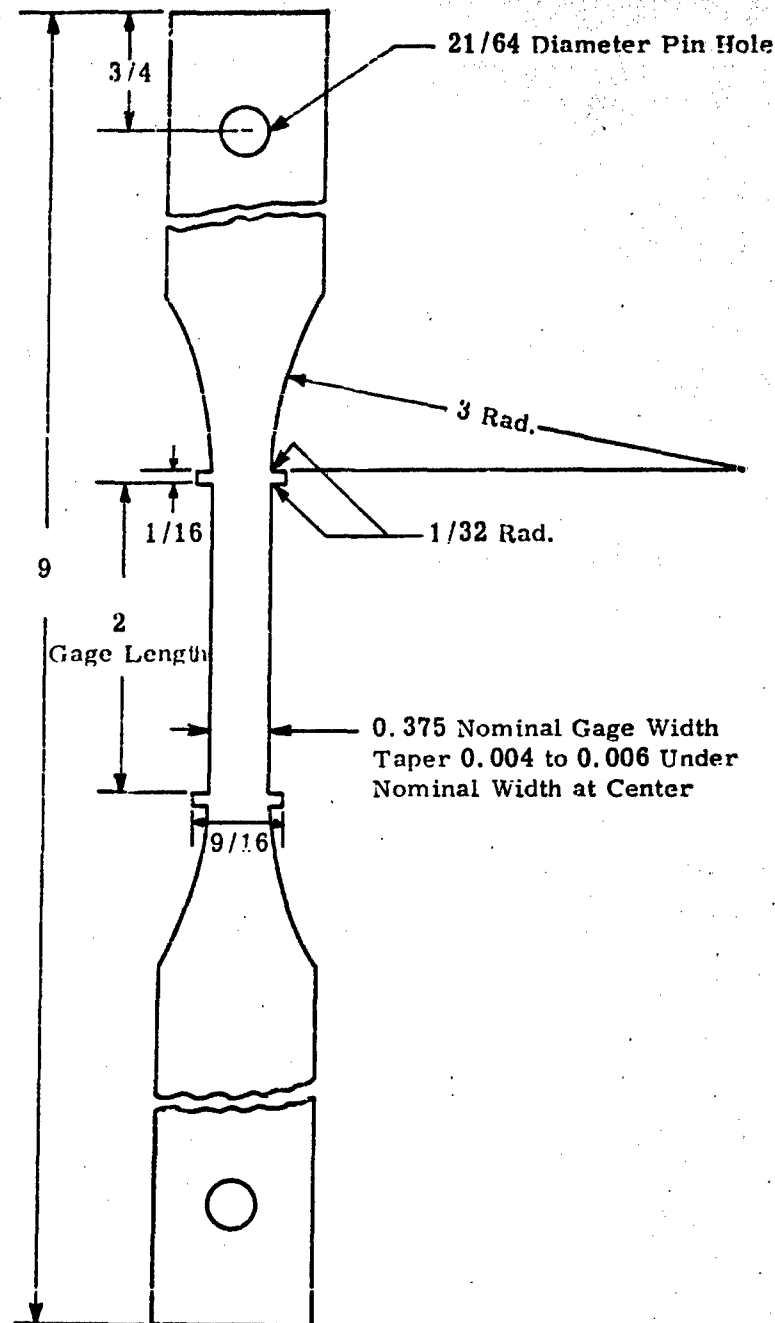


Figure 1. Sheet Tensile Specimen

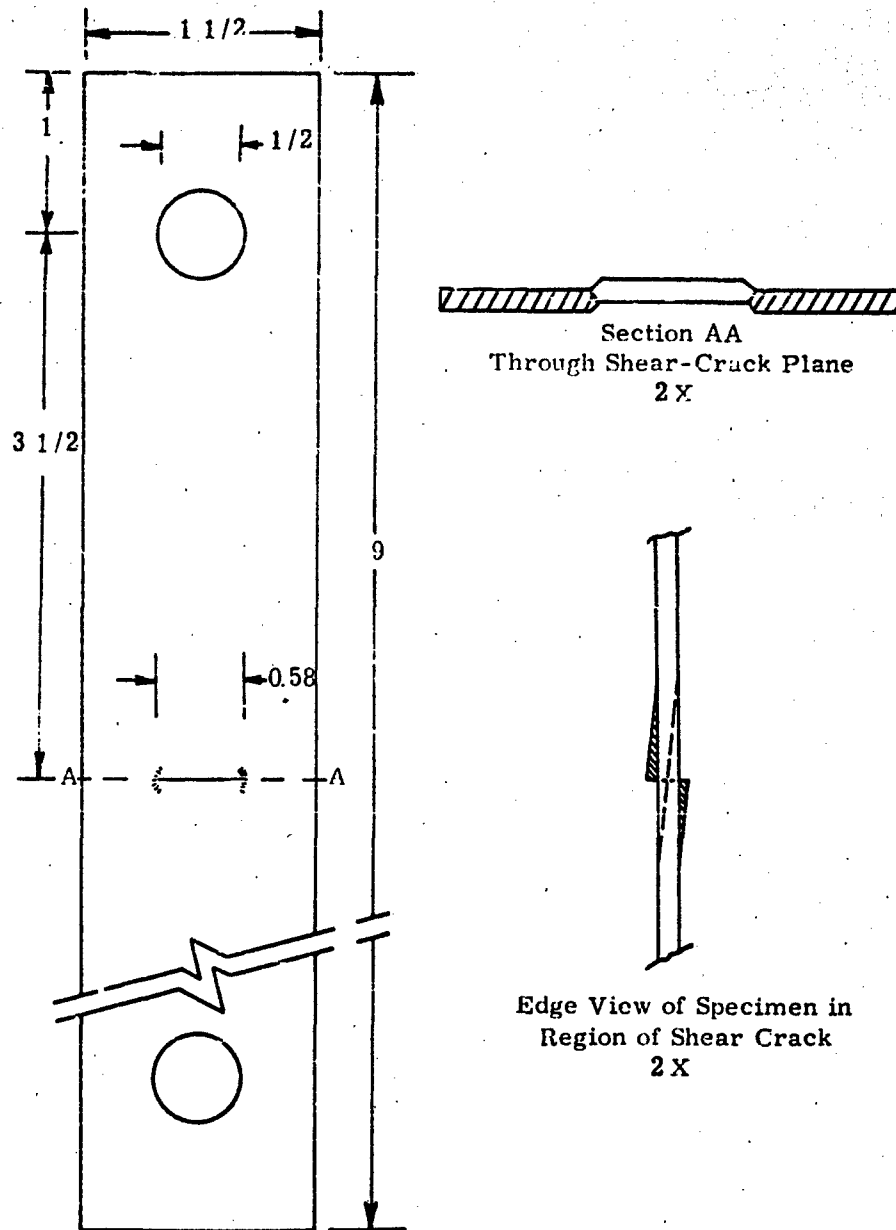


Figure 2. Typical shear-cracked specimen

in. For sheet thicknesses in excess of 0.080 in., specimens 2.65 in. wide were used, with a shear-crack length of 1.05 in.<sup>2</sup> These dimensions met the requirements established by the ASTM Committee on Fracture Testing of High Strength Sheet Materials (1) for width-to-thickness ratio and for crack-length-to-specimen-width ratio. The crack-propagation specimens of quench-hardenable and age hardenable materials were shear-cracked in the annealed condition and were then heat treated.

The model pressure vessels used in the comparative program were obtained in the heat-treated condition from the Kidde Aero-Space Division. The AISI 4130 steel vessels were 205-cu-in. seamless (cold-drawn) gas cylinders, 5 210 in. in diameter, with a wall thickness of 0.105 in. The dimensions of a typical 4130 steel cylinder are shown in Figure 3. Because of the limited amount of sheet stock available, the 4340 steel vessels were formed to a smaller diameter (3.52 in.) than the 4130 steel vessels.

#### C. Equipment and Procedure

A special screw-type tensile loading machine, designed and built at Southern Research Institute, was used for determining the standard tensile properties of the sheet materials (and for the crack-propagation specimens when rapid strain rates were required). With this machine, a range of strain rates of from 0.00005 in./in./sec to 1.0 in./in./sec can be obtained for standard tensile specimens of 2 in. gage length. Usually, the standard specimens were loaded to failure at a strain rate of 0.0001 in./in./sec. Both the load cell and the extensometer use strain gages to produce electrical signals proportional to the load and to the strain within the 2-in. gage section of the specimen. The recorded stress-strain curves were photographed by a Polaroid-Land camera from a cathode-ray oscilloscope. Most of this equipment was developed during the past seven years under several research contracts sponsored by the U. S. Air Force. A detailed description of the equipment is contained in WADC TR 57-649.

<sup>2</sup> The one exception was the 4340 steel sheet used to obtain crack-propagation data for comparison with the burst properties of the 4340 steel vessels. Because of the very small amount of sheet stock available, the crack propagation specimens prepared from this 0.120 in.-thick stock were 1.87 in. wide.



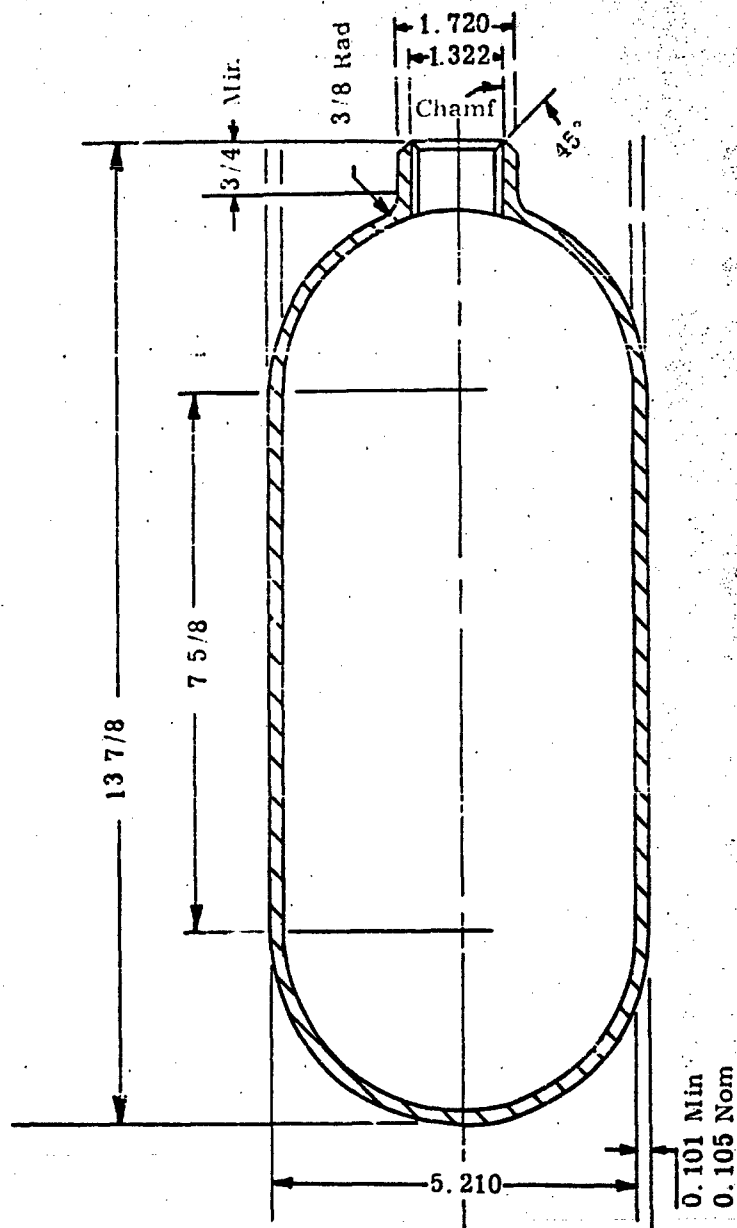


Figure 3. Longitudinal section of model pressure vessel used for determining burst properties of AISI 4130 steel. Vessels fabricated from AISI 4340 steel were similar but were 3.52 in. in diameter.

The crack-propagation specimens were usually loaded to failure in a Tinius Olsen tensile machine at a free crosshead-travel rate of about 0.01 in./min. This rate caused fracture within 2 to 4 min. When it was desired to determine fracture properties at very high rates of loading, the crack-propagation specimens were fractured in the SRI tensile machine.

The desired specimen temperature was obtained in the following ways for both the standard tensile specimens and the crack-propagation specimens. For the low-temperature work, the central 3-in. section of the specimen was enclosed in an insulated cold-box that was continuously swept with cold nitrogen gas. The nitrogen gas was cooled by passing it through a heat-exchange coil immersed in liquid nitrogen. With this system, specimen temperatures as low as  $-250^{\circ}\text{F}$  could be attained. For the elevated-temperature work, the specimens were heated and then maintained at a constant uniform temperature by two focused radiant-heating fixtures. Both surfaces of the specimens were uniformly flooded with radiant energy from G. E. Type 500 T3/CL tubular infrared lamps with clear quartz envelopes. The output from a single lamp in each reflector was concentrated upon the surface of the specimens by a focused reflector in the form of a three-quarter section of an elliptic cylinder.

Temperature control was effected by means of a 36-gage chromel-alumel thermocouple, flash-welded to the specimen and connected to a temperature controller working in conjunction with the radiant lamps for the elevated-temperature work, or in conjunction with a solenoid valve in the nitrogen-gas line for the low temperature work.

With the equipment described, standard tensile properties and crack-propagation properties could be determined at any temperature from about  $-250^{\circ}\text{F}$  to  $1200^{\circ}\text{F}$ .

The equipment for determining the burst strengths of the model pressure vessels consisted of a hydraulic hand-pump connected to the vessel by means of special high-pressure tubing and fittings. The system pressure was read on a bourdon-tube gage, which was calibrated by means of a dead-weight gage tester. For the evaluations at room temperature, hydraulic-pump oil was used as the pressurizing medium. For the low-temperature work, trichlorethylene was used as the hydraulic medium, and the vessel was immersed in a bath of trichloroethylene and dry ice. For temperatures below the equilibrium

temperature of the dry-ice bath ( $-105^{\circ}\text{F}$ ), additional cooling was effected by means of a heat-exchange coil in the bath, liquid nitrogen being introduced into the coil until the desired temperature was reached. For the elevated-temperature work, the pressurizing medium was a high-flash-point turbine oil, which was also used in the bath surrounding the vessel. The oil-bath was heated with immersion heaters.

#### D. Electrical Measurement of Slow-Crack Extension

As has been previously noted, the most direct method of calculating the critical fracture-toughness parameter,  $K_{IC}$ , depends upon knowing the crack length at the onset of rapid crack-extension. Probably the most widely used method of determining this critical crack length has been to stain the fracture surfaces formed during slow crack-extension. However, there are objections to the use of the staining method. First, the application of the ink-staining method is limited to near-ambient temperature environments. And second, there is recent evidence that the presence of aqueous materials in the slowly extending crack lowers the fracture strength of the material (3).

In the course of this program, an electrical method of measuring slow-crack extension was developed, and some preliminary experimental work was done using this method. In the electrical method, a regulated direct current of low amperage (10 amps) was passed through the specimen, and the potential-drop across the crack was recorded as a function of time as the specimen was loaded to failure. Connection to the recording-potentiometer input was made by 36-gage wires flash welded to the specimen at points in the center of the specimen width and on opposite sides of the crack. Calibration standards for the method were specimens of the same material as the experimental samples and containing cracks of known length.

One limitation to this method of determining crack length is that the method should be applied only to specimens that are in fairly brittle condition, in which there is no general plastic flow across the net supporting section. This brittle state often implies a low-temperature environment, and it is probable that the electrical method is most useful for specimens fractured at low temperatures.

The cursory investigation of the electrical method for measuring critical crack-length was made in conjunction with the evaluation of

shear-cracked specimens of AM 350 and AISI 4130. Some " $K_{C1}$ " data obtained by means of this method will be shown in the results for the 4130 steel.

#### IV. EXPERIMENTAL RESULTS

The experimental results for the entire program are presented the four general sections which follow. In the first section, crack-propagation properties (as obtained with shear-cracked specimens) and comparative standard tensile properties of each sheet material are presented. For the low-alloy steels and stainless steels, these properties have been obtained as a function of temperature, at a slow rate of loading. For the aluminum alloys, it was necessary to use very specialized conditions of heating and loading to obtain the desired data, and these data are given in a separate sub-section.

Some of these basic data reported in the first section, A, entitled "Evaluation of Crack-Propagation Characteristics of Sheet Materials," will again be utilized for comparative purposes in subsequent sections which deal with; B) correlation of crack-propagation data with burst strengths of model pressure vessels, C) effects of several experimental variables on crack-propagation properties, and D) comparison of results obtained with different types of crack-propagation specimens.

##### A. Evaluation of Crack-Propagation Characteristics of Sheet Materials

##### 1. Low-Alloy Steels and Stainless Steels

The results of the evaluations of the low-alloy steels and stainless steels are presented in tables and graphs which are identified as follows:

<u>Sheet Material</u>	<u>Properties</u>	<u>Table No.</u>	<u>Figure No.</u>
AMS 6434	Standard tensile	3	4
AMS 6434	Crack-Propagation	4	4 & 5
300M	Standard tensile	5	6

Sheet Material	Properties	Table No.	Figure No.
300 M	Crack-propagation	6	6
301 (50% CR)	Crack-propagation	7	7
AISI 4130 (0.040 in. thick, 240,000 psi level)	Standard tensile	8	8
	Crack-propagation	9	8
AM 350	Standard tensile	10	9
	Crack-propagation	11	9
17-7 PH	Standard tensile	12	10
	Crack-propagation	13	10
AISI 4130 (0.100 in. thick 200,000 psi level)	Standard tensile	14	11
	Crack-propagation	15	11 & 12
AISI 4130 (0.100 in. thick, 240,000 psi level)	Standard tensile	16	13
	Crack-propagation	17	13
AISI 4340 (0.064 in. thick)	Standard tensile	18	14
	Crack-propagation	19 & 19A	14
Inconel-X	Standard tensile	20	15
	Crack-propagation	21	15
AISI 4340 (vacuum remelted) (0.120 in. thick)	Crack-propagation	22	16

The data tables are included in Appendix A. The figures showing comparative standard tensile properties and crack-propagation properties for each of the steels, together with a short discussion of the results, are presented in the following pages. It should again be noted that the crack propagation specimens used to obtain these data were shear-cracked specimens of either 1.5 in., 1.87 in., or 2.65 in. over-all width, depending upon sheet thickness. These specimens were loaded to failure slowly at various temperatures, fracture occurring in from 2 to

4 min after loading was initiated. The crack-propagation data shown in the figures are net fracture stress<sup>3</sup> (or, identically, notch tensile strength) and the percent shear in the fracture surface. This percent shear value is defined as the percent of the specimen thickness represented by shear-borders in the fracture surface, as measured at a point from one to two times the specimen thickness from the end of the specimen.

For one material, AISI 4130 sheet (0.100 in. thick, 200,000 psi strength level),  $K_{C3}$  values are plotted in Figure 12 as a function of temperature. Two values of  $K_{C1}$  obtained with the aid of the electrical method of measuring critical crack length, are also plotted in Figure 12. For many of the sheet materials evaluated,  $K_{C3}$  values are shown in the data tables, Appendix A, along with the other properties, net fracture stress and fracture appearance.

---

<sup>3</sup> The use and limitations of net fracture stress as an indication of crack-propagation resistance have been reviewed in detail by J. E. Srawley (2).

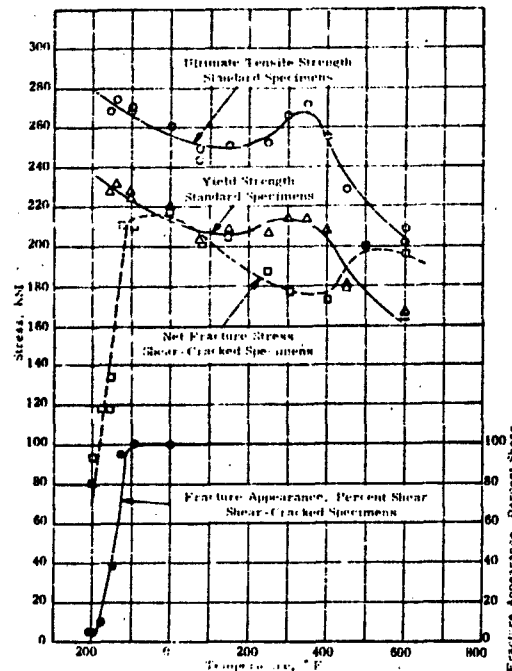


Figure 4 Effect of temperature on the standard tensile properties and fracture properties of heat-treated longitudinal specimens of AMS 6434 steel sheet

\* Austenitized at 1620° F for 30 min (argon), oil-quenched; double tempered at 400° F for 2 hr.

The standard tensile properties and fracture properties of the AMS 6434 steel are compared in Figure 4 for the temperature range from -200° F to 600° F. The fracture surfaces of the specimens are shown in Figure 5. The full-shear transition temperature for this material was -100° F. The transition temperature as indicated by the net fracture stress is in good agreement with the full-shear transition temperature. For the standard tensile specimens, both the 0.2%-offset yield stress and the ultimate tensile stress show a marked "maximum" at about 350° F. This maximum correlated with a decrease in net fracture stress. It is believed that these effects are a result of strain aging.

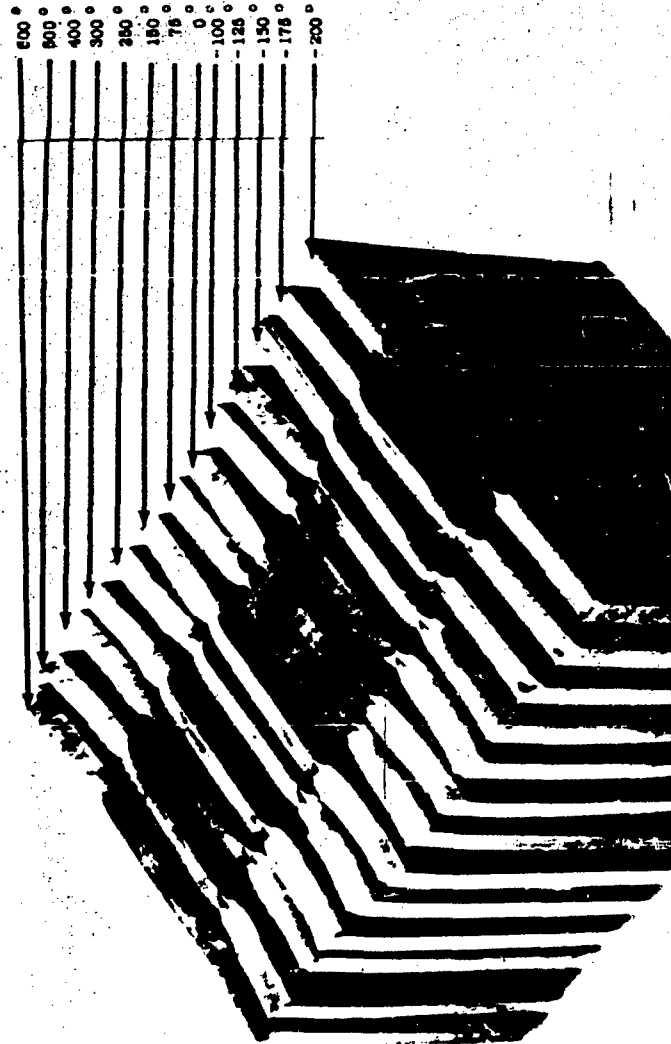


Figure 5. Appearance of fracture surfaces of shear-cracked AMS 3434 steel sheet loaded to failure at temperatures from -200° F to 600° F.



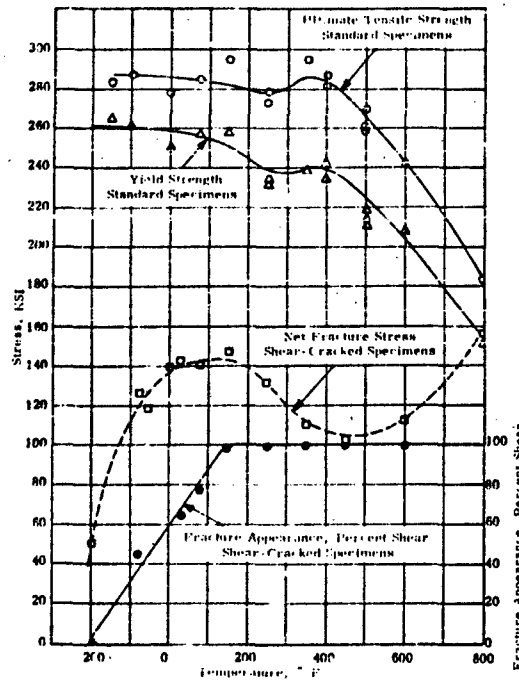


Figure 6 Effect of temperature on the standard tensile properties and fracture properties of heat-treated longitudinal specimens of 300 M steel sheet

Heat-treated at 1600°F for 30 min (air-cooled), oil-quenched, double tempered at 600°F for 3 hr each cycle.

The standard tensile properties and crack-propagation properties of the 300 M alloy are shown in Figure 6, for the temperature range from -200°F to 800°F. This alloy has a less well defined fracture-appearance transition temperature than does the AMS 6434 steel, and the net fracture stress does not approach the yield strength below 800°F. This is a marked drop in net fracture stress in a broad temperature range from about 250°F to 700°F, which effect may be associated with the strain-aging "maximum" shown in the standard tensile properties.

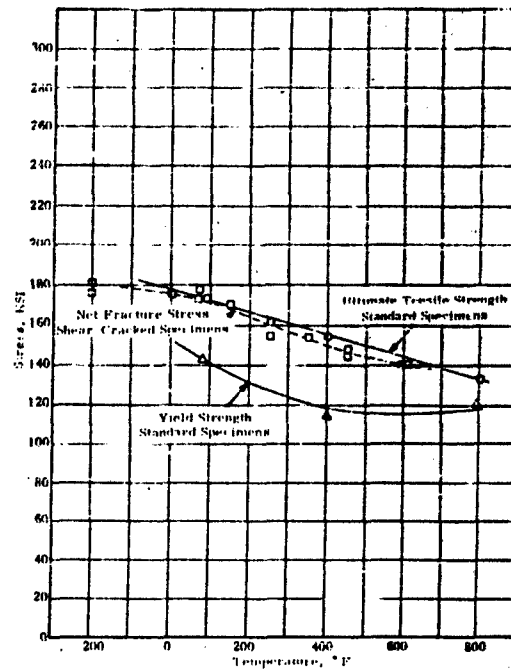


Figure 7. Effect of temperature on the standard tensile properties and fracture properties of longitudinal specimens of full-hard<sup>a</sup> Type 301 stainless steel sheet.

<sup>a</sup> 50% cold reduced

The standard tensile and crack-propagation properties of Type 301 full-hard (50% cold-reduced) stainless steel sheet are compared in Figure 7. These properties were obtained for the temperature range from -200° F to 600° F. The shear-cracked specimens of this material had considerable ductility even at the lowest temperature (-200° F), and the net fracture stress corresponded closely to the ultimate tensile strength over the entire temperature range, being highest at -200° F.

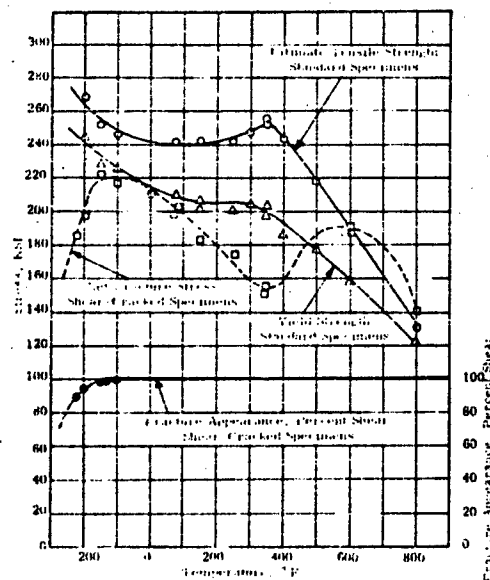


Figure 8. Effect of temperature on the standard tensile properties and fracture properties of heat-treated, longitudinal specimens of AISI 4130.

\* Annealed at 1570°F for 30 min (air cool), oil quenched, tempered at 400°F for 2 hr.

In Figure 8 is shown a comparison of the standard tensile properties and crack-propagation properties of 0.040-in. -thick AISI 4130 sheet, heat treated to a nominal strength level of 240,000 psi (tempered at 400°F). This tempering treatment resulted in the rather low transition temperature of about -150°F for the 4130 sheet. Again, the "strain-aging effect" was evident, there being a maximum in ultimate tensile strength and a minimum in sharp-notch strength at 350°F.

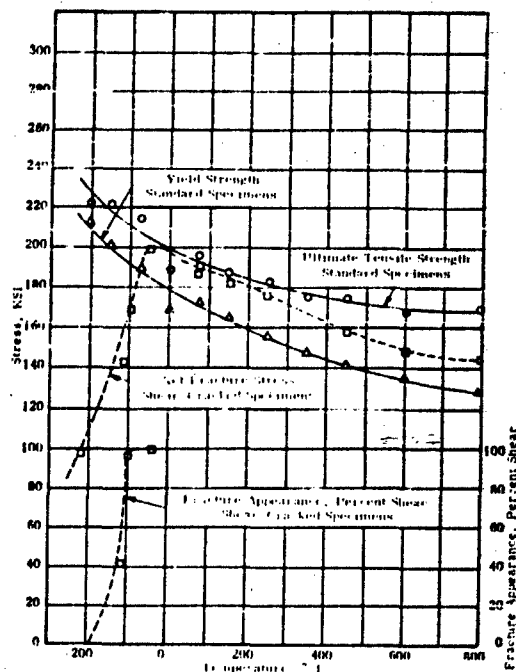


Figure 9 Effect of temperature on standard tensile properties and fracture properties of heat-treated<sup>1</sup> longitudinal specimens of AM 350 sheet, loaded to fracture in 2 min.

<sup>1</sup> Solution treated at 1750°F for 30 min (argon), water quenched; reheated at 1050°F for 3 hr; aged at 850°F for 3 hr.

Figure 9 shows a comparison of the standard tensile properties and fracture properties of AM 350 sheet (0.040 in. thick) in the SCT (850) condition. This material had a transition temperature of -50° F, on the basis of net fracture strength, and -100° F, on the basis of fracture appearance.

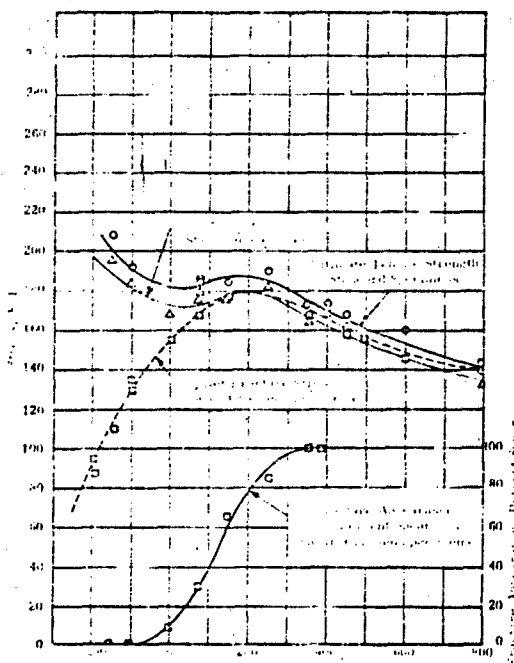


Fig. 1. Standard tensile properties and fracture properties of 0.040 in. thick 17-7 PH sheet in the TH 1050 condition. The fracture data obtained with shear-cracked specimens indicated a rather indefinite fracture-appearance transition range, with a full shear temperature of about 300°F. The net-fracture strength data also showed a fairly broad and poorly defined transition range.

17-7 PH (UNS S17700) - 0.040 in. thick - TH 1050 condition

This figure shows standard tensile properties and fracture properties of 0.040 in. thick 17-7 PH sheet in the TH 1050 condition. The fracture data obtained with shear-cracked specimens indicated a rather indefinite fracture-appearance transition range, with a full shear temperature of about 300°F. The net-fracture strength data also showed a fairly broad and poorly defined transition range.

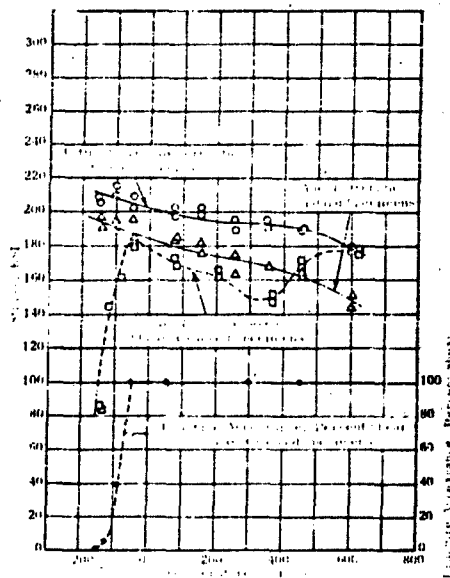


Figure 11. Standard tensile properties and crack-propagation properties of 0.100-in. thick AISI 4130 steel sheet, tempered at 825°F.

Heat-treated at 1700°F for 6h and tempered at 825°F for 1h.

Figure 11 shows the standard tensile properties and crack-propagation properties of 0.100-in. thick AISI 4130 steel sheet at the 200,000 psi strength level (tempered at 825°F). For this material, there was a sharp brittle-ductile transition, as shown by fracture strength and fracture appearance, at a temperature of -50°F. There was also evidence of strain-aging effects at 300-350°F. These data will be utilized in a subsequent section for comparison with the burst properties of model pressure vessels fabricated from 4130 steel and tempered to the same strength level (200,000 psi).

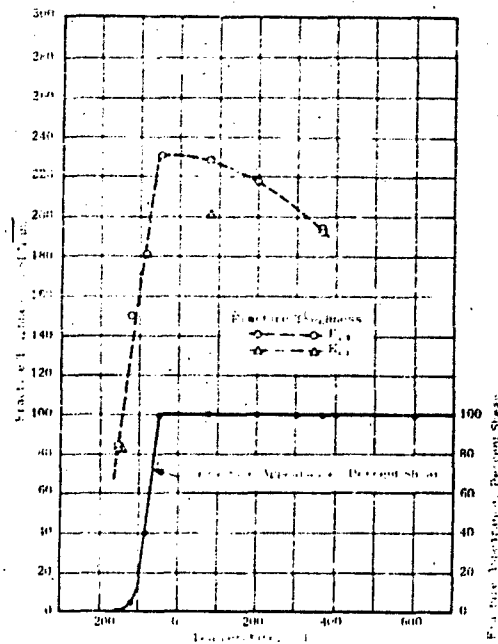


Figure 12. Fracture toughness and fracture appearance of AISI 4130 steel at 200,000 psi strength level.

Fracture toughness was determined by the  $K_{C1}$  method. Fracture appearance was determined by the percent shear method.

In Figure 12 are plotted values of fracture appearance and fracture toughness,  $K_{C1}$ , as a function of temperature for the AISI 4130 steel at the 200,000 psi strength level. The values were calculated from the maximum load data, the initial crack-length values, and the fracture-appearance data for the shear-cracked specimens. For two specimens, one fractured at room temperature and one at  $-150^{\circ}\text{F}$ ,  $K_{C1}$  values were calculated from critical crack lengths measured by the ink-stain method or by the electrical resistance method. The brittle-ductile transition temperature of this material was shown to be  $-50^{\circ}\text{F}$  by the fracture-toughness criterion as well as by the fracture-strength and fracture-appearance criteria.

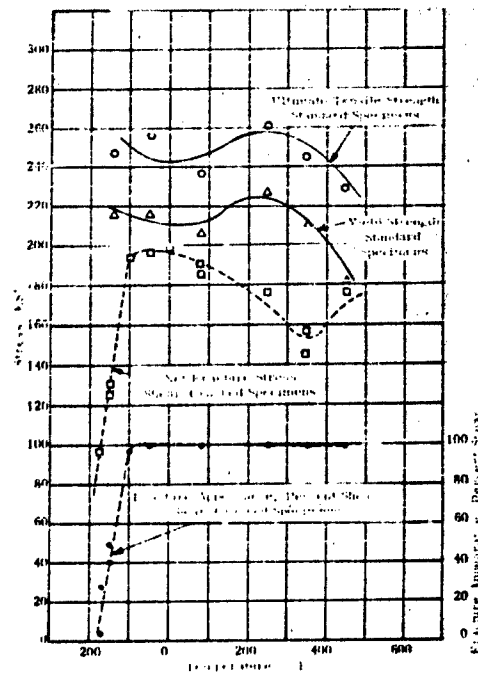


Figure 13. Effect of temperature on the standard tensile strength and fracture appearance of AISI 4130 steel specimens.

<sup>1</sup> Heat treated by solution annealing at 1700°F for 60 min. and tempering at 400°F for 1 hr.

Here is shown a comparison of the standard tensile properties and crack-propagation properties of 0.100-in.-thick AISI 4130 steel sheet, heat treated to 240,000 psi nominal tensile strength level (tempered at 400° F). The transition temperature of this material was -100° F, and there was a pronounced strain-aging maximum in smooth tensile-strength values that coincided with a drop in fracture strength at about 350° F. These data, obtained with sheet specimens, will also be presented graphically in a later section which compares the properties of sheet specimens with the burst properties of model vessels.



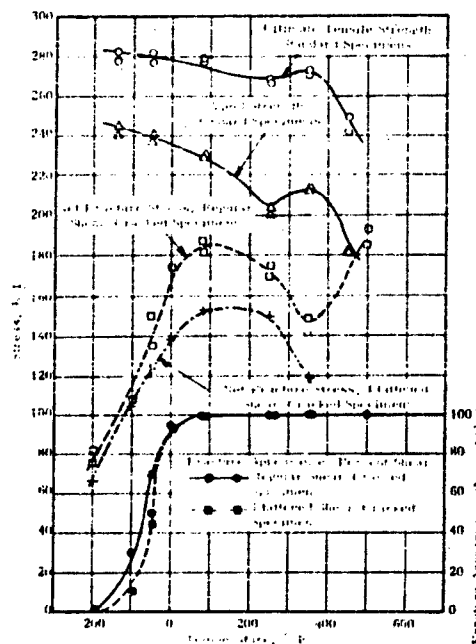


Figure 14 Effect of temperature on the ultimate tensile strength, yield strength, and fracture properties of AISI 4340 steel sheet specimens. The specimens were heat treated to a nominal strength level of 280,000 psi (tempered at 400° F).

Figure 14 shows the results of an evaluation made of 0.063-in.-thick AISI 4340 steel sheet specimens for standard tensile properties and fracture properties. This material was heat treated to a nominal strength level of 280,000 psi (tempered at 400° F). Two sorts of shear-cracked specimens were used: the usual type—as appears in Figure 2, and a few specimens that were "flattened" after shear-cracking to remove the protrusions and the discontinuity in the shear plane. Both types of shear-cracked specimens indicated the same rather broad transition range. The best estimate of a "transition temperature" is about 75° F, on the basis of the two criteria, net fracture stress and fracture appearance. The "strain-aging effect," at a temperature of about 350° F, was quite pronounced. The "flattened" specimens were slightly more sensitive—showed lower net fracture stress—than the "standard" shear-cracked specimens.

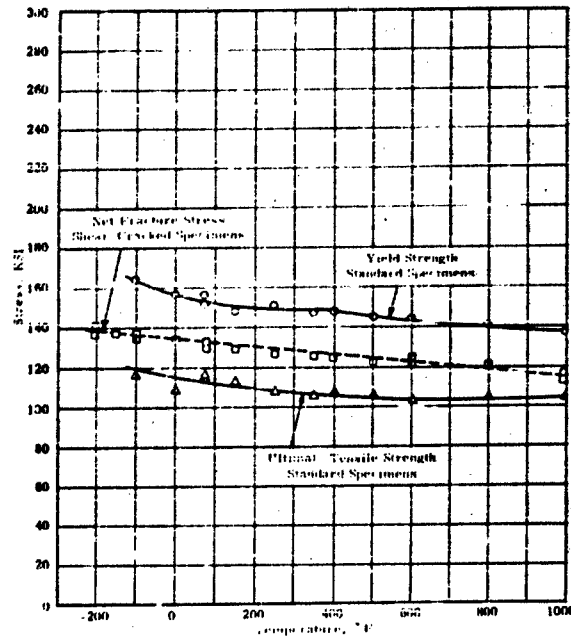


Figure 15 Effect of temperature on the standard tensile properties and the net fracture strength of aged Inconel-X sheet.

<sup>1</sup> Aged at 1300°F for 20 hr.

Figure 15 shows a comparison of the standard tensile properties and crack-propagation properties of 0.064-in. -thick Inconel-X sheet, aged at 1300°F for 20 hr. As is evident in this figure, the Inconel-X is quite notch-insensitive over the wide temperature range from -200°F to 1000°F.

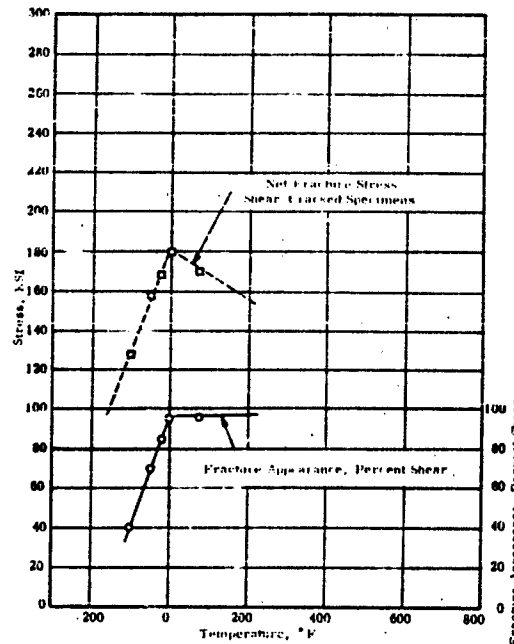


Figure 10 Effect of temperature on the net fracture stress and fracture appearance of shear-cracked AISI 4340 sheet specimens. Specimens were 1.87 in. over-all width and 0.120 in. thick.

<sup>4</sup> Hardened, and tempered for 2 hr at 425° F

This figure shows the results of an evaluation of shear-cracked specimens of 0.120-in.-thick, vacuum remelted, AISI 4340 sheet, oil-quenched from 1600° F and tempered 2 hr at 425° F.<sup>4</sup> Because of the limited amount of sheet stock available, no standard tensile specimens were prepared; the shear-cracked specimens used were 1.87 in. wide. The crack-propagation transition temperature for this material, as shown by a sharp decrease in net-fracture stress and in percent shear, is about 0° F. These data will again be used to compare with burst properties of 4340 steel model vessels, at the same strength level.

<sup>4</sup> This material was decarburized at some point in the production of the sheet, and the nominal strength level obtained by the indicated heat treatment was in the range of 240,000-262,000 psi

## 2. Aluminum Alloys

Aircraft structures, fabricated from aluminum alloys, may be exposed to certain service conditions that impose sudden heating and stressing. Information is needed on the resistance to crack-propagation of aluminum structural sheet alloys under these simulated service conditions. Four aluminum alloys—7075-T6, 7079-T6, 2024-T86, and X2020-T6—have been evaluated to determine the effects on fracture properties of very rapid stressing following two different heating conditions—heating very rapidly to temperature and immediately loading to failure or heating to temperature and holding for 30 min before loading. Both standard tensile properties and fracture properties were determined for each experimental condition.

The standard tensile specimens and crack-propagation specimens were prepared from 0.063-in. thick sheet samples of the four alloys, which were obtained in the heat-treated condition from the Aluminum Company of America. The shear-cracked specimens were 1.5 in. in over-all width, the crack-length to specimen-width ratio being about 0.38.

The experimental conditions used for each alloy were as follows: temperatures of 75° F, 200° F, 300° F, and 400° F; holding times at temperature (before loading) of 0 sec and 1800 sec; time to reach temperature—4 sec; strain rate of 0.1 in./in./sec. This strain rate was such that the 0.2%-offset yield strength of standard tensile specimens was reached in 0.1 sec or fracture of the crack-propagation specimens was produced in about 0.1 sec.

The specimens were loaded to failure in the Southern Research Institute rapid tensile machine. Heating was effected by means of radiation lamps, which were regulated by thermocouples flash-welded to the specimen and operating through a temperature controller.

Fracture properties were determined for all conditions of temperature and holding time with shear-cracked specimens.

All of the data are presented in tables and graphs as shown below:

<u>Alloy</u>	<u>Properties</u>	<u>Table No.</u>	<u>Figure No.</u>
7075-T6	Standard tensile	23	17
7075-T6	Crack-propagation	24	17

<u>Alloy</u>	<u>Properties</u>	<u>Table No.</u>	<u>Figure No.</u>
7079-T6	Standard tensile	25	18
7079-T6	Crack-propagation	26	18
2024-T86	Standard tensile	27	19
2024-T86	Crack-propagation	28	19
X2020-T6	Standard tensile	29	20
X2020-T6	Crack-propagation	30	20

These data tables are given in Appendix A. The figures (17-20) showing comparative standard tensile properties and crack-propagation properties for each of the aluminum alloys, with a discussion of the results, follow immediately. (In a subsequent section, a comparison will be shown of crack-propagation properties obtained with the shear-cracked specimens and with fatigue-cracked specimens of the four aluminum alloys, loaded to failure in 0.1 sec.)

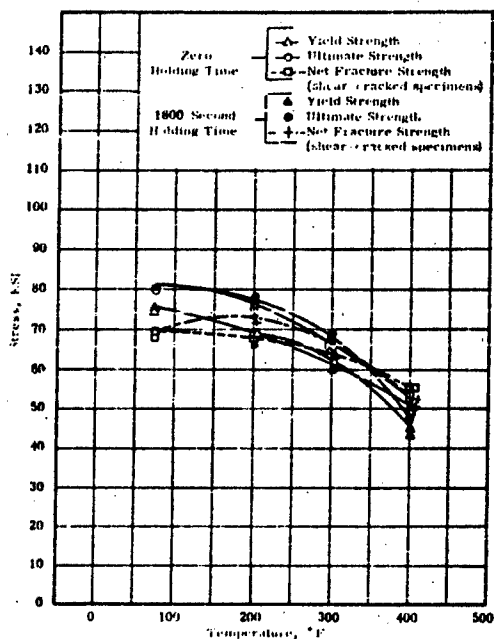


Figure 17 Effect of holding time after rapid heating on the tensile properties and fracture strength of 7075-T6 aluminum sheet loaded rapidly to failure at different temperatures

As is shown in Figure 17, the standard tensile properties of the 7075-T6 alloy decreased steadily with increasing temperature. In the range from 200° F to 300° F, ultimate strength of the samples held for 1800 sec at temperature before loading was slightly higher than the zero-holding-time specimens, but at 400° F this trend reversed probably as a result of over-aging. At room temperature, the fracture strength was somewhat below the yield strength, reflecting a moderately brittle condition of this alloy. As the temperature was increased above 75° F, the fracture strength approached the yield strength, and at about 250° F, the full yield strength of the material was realized even in the presence of the crack-like defects represented by shear cracks. The fracture strength of the shear-cracked specimens held for 1800 sec at temperature before loading increased with increasing temperature.

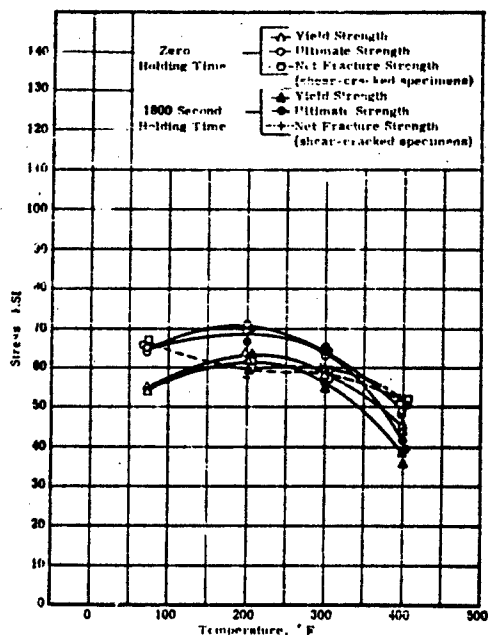


Figure 18. Effect of holding time after rapid heating on the tensile properties and fracture properties of 7079-T6 aluminum alloy loaded rapidly to failure at different temperatures.

Figure 18 shows the comparison of properties for the 7079-T6 alloy. The standard tensile-strength properties of the 7079-T6 showed a slight maximum at 200° F that coincided with a slight dip in net fracture strength. At all temperatures, however, the net fracture strength was very close to, or in excess of, the yield strength. No pronounced effects of holding time were evident for the 7079-T6 material, with the exception of an indication of apparent over-aging at 400° F.

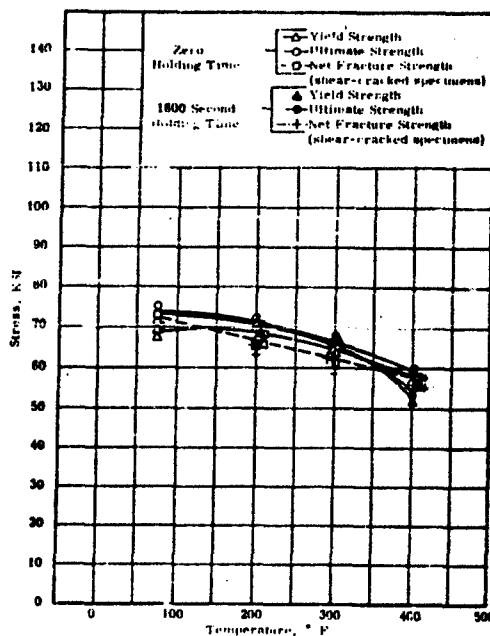


Figure 19 Effect of holding time after rapid heating on the tensile properties and fracture strength of 2024-T86 aluminum sheet loaded rapidly to failure at different temperatures.

Figure 19 shows the comparison of tensile and fracture properties for the 2024-T86 aluminum. Increasing temperature produced a moderate and almost linear decrease in standard strength properties of this material. Fracture strength, which was above the yield strength at room temperature, fell below the yield strength in the range from 200° F to 300° F and was equal to the yield strength at 400° F. There were no pronounced effects of holding time on the strength properties of this alloy at temperatures up to 300° F, but at 400° F there was a slight amount of over-aging as indicated by the decrease in yield and ultimate strength with increasing holding time.



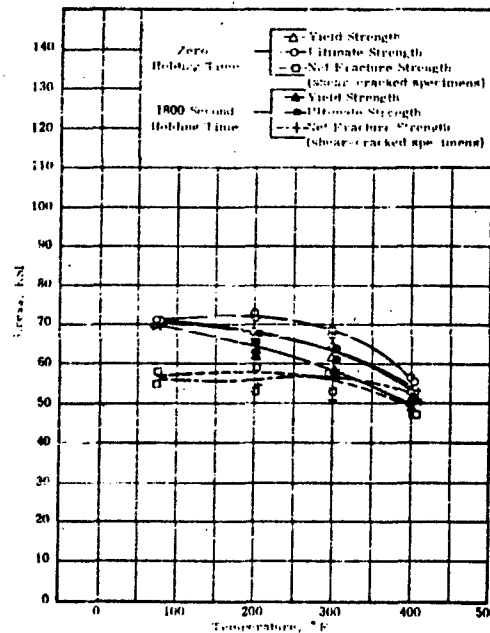


Figure 20 Effect of holding time after rapid heating on the tensile properties and fracture strength of X2020-T6 aluminum alloy. Effect on yield strength at different temperatures.

The tensile and fracture properties of X 2020-T6 are shown in Figure 20. The reduction of tensile strength properties resulting from 30 min holding time at temperature was slightly more pronounced in the X 2020 T6 alloy than in the other aluminum alloys. The fracture strength, which was not appreciably affected by holding time, was well below the yield strength at temperatures below about 400° F. The X 2020-T6 was, on this basis, the most "brittle" of the four alloys.

#### B. Evaluation of Model Pressure Vessels

The ultimate aim of the crack-propagation test is to predict the service performance of missile motor cases and other structures exposed to complex stress states. One important phase of this investigation has been concerned with correlating crack-propagation properties, as measured with cracked specimens, with burst properties of model pressure vessels fabricated of the same material. Two high-strength steels were used in this investigation—AISI 4130 and AISI 4340. The model vessels fabricated from these steels were seamless, having been formed entirely by drawing and spinning techniques. In such form, the vessels contained no stress-concentrating defects such as are often produced by joining operations. Therefore, the burst properties of these vessels, in which the effects of fabrication were kept to a minimum, represented more nearly the inherent biaxial strengths of the materials themselves.

The maximum hoop-stress values and fracture appearance data for the model vessels are given in the data tables and graphs as shown:

<u>Vessel Material</u>	<u>Table No.</u>	<u>Figure No.</u>
AISI 4130 - 200,000 psi strength level	31	21 & 22
AISI 4130 - 240,000 psi strength level	32	23
AISI 4340 - 240,000 - 262,000 psi strength level	33	24 - 27

The data tables appear in Appendix A. The figures, showing burst properties of the vessels and tensile and fracture properties of the comparative sheet specimens plotted as functions of temperature are presented in the following sections. Brief discussions of the results are also given, and photographs of some of the fractured vessels are shown.

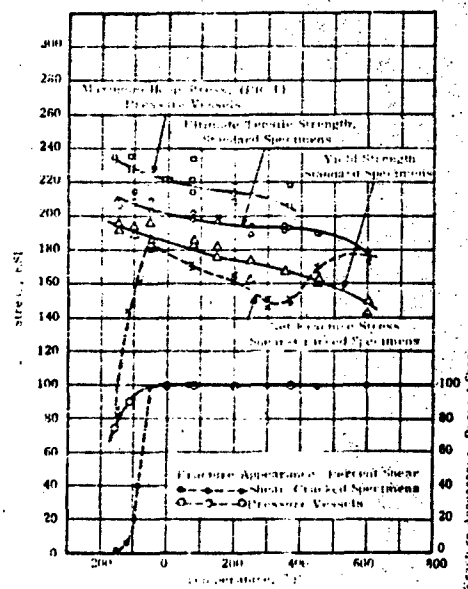


Figure 21 Effect of temperature on the fracture properties of AISI 4130 steel vessels and on the standard tensile specimens of AISI 4130 steel sheet specimens.

Heat treatment as follows: Annealed at 1700°F for 50 min and quenching temperature at 825°F for 1 hr.

Figure 21 shows the burst strength and fracture appearance data for the 200,000 psi strength level AISI 4130 steel vessels and the standard-tensile and crack-propagation data obtained with sheet specimens of the same nominal strength level. Hoop stress at burst generally decreased with increasing temperature, and no fracture-stress transition temperature was evident for the vessels.

As is shown in Figure 22, the 4130-steel vessels, in this ductile condition, deformed considerably before fracture, particularly at room temperature and at elevated temperatures. In the vessels fractured at -105° F and -160° F, the fractures extended into or completely through the end closures, indicating that some rapid, low-energy extensions of the fractures occurred at those temperatures. These fractures that extended into the thicker end-closure regions were characterized by increasing tendency toward brittle fracture, becoming fully brittle (flat tensile) in the thickest portions of the end closures.

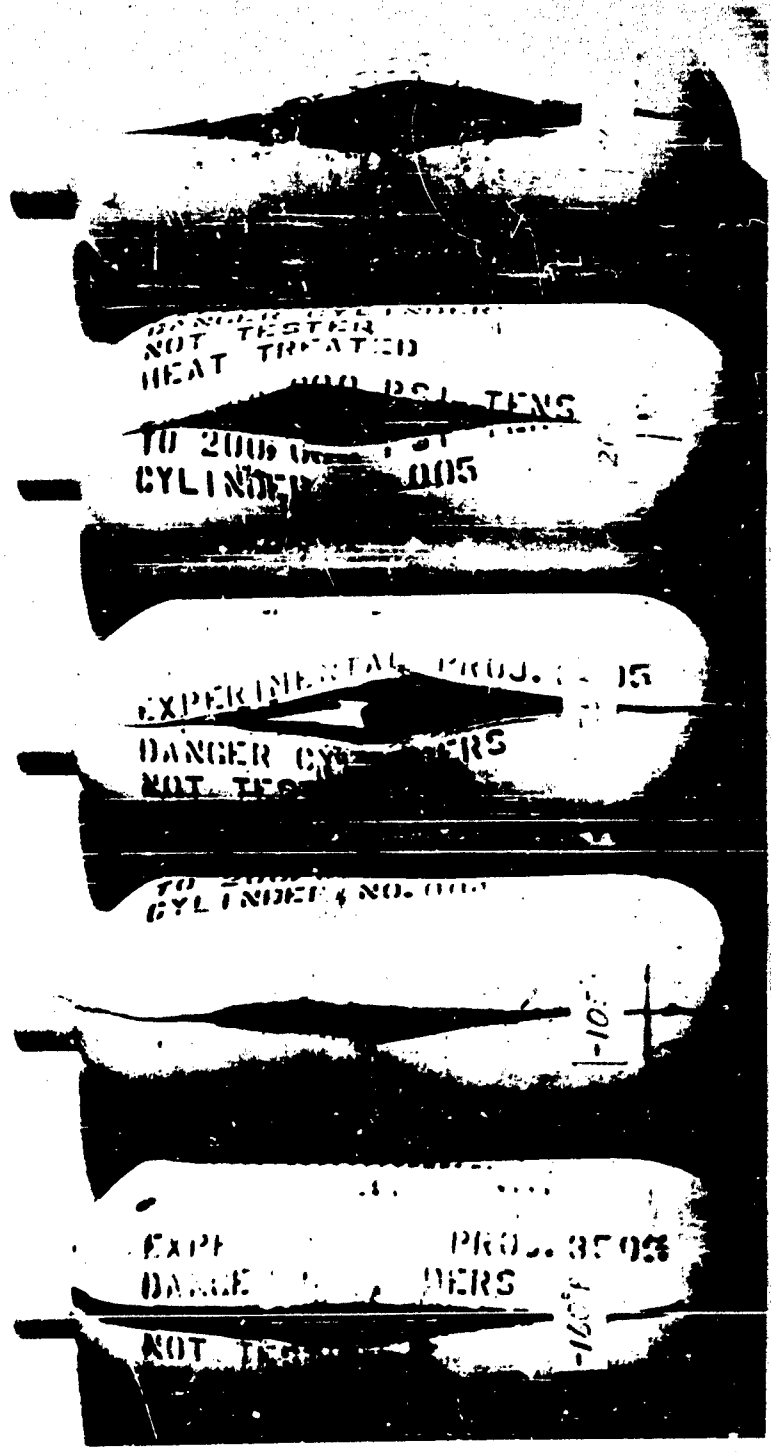


Figure 22. Typical model vessels of AISI 4130 steel, heat treated to 200,000 psi strength level, fractured at temperatures from -160° F to 365° F.

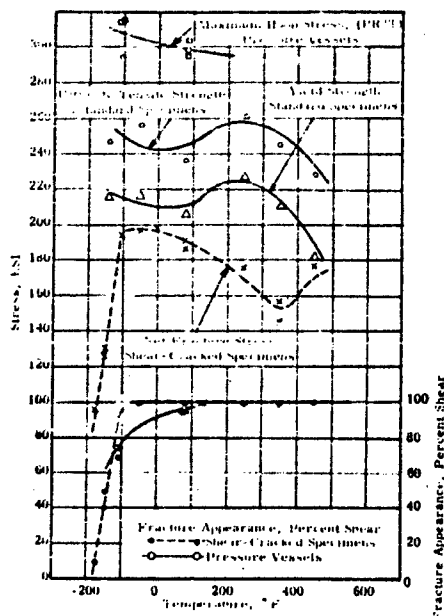


Figure 23 Effect of temperature on the burst properties of AISI 4130 steel vessels<sup>1</sup> and on the standard tensile properties and fracture properties of AISI 4130 steel tensile specimens.

<sup>1</sup> Heat treated as follows: Austenitized at 1700°F for 60 min, oil quenched, and tempered at 400°F for 1 hr.

Data presented previously (Figure 8) have shown that AISI 4130 steel (0.040-in. -thick sheet) heat treated to 240,000 psi strength level (tempered at 400°F) has good fracture toughness and a low transition temperature, -150°F. In view of these properties, it was thought advisable to evaluate a few 4130 steel vessels at the 240,000 psi strength level to determine the biaxial properties of this material. The results of this evaluation and the comparative properties of shear-cracked specimens and standard tensile specimens, prepared from 0.100-in. -thick sheet, are shown in Figure 23. On the basis of these few data, it is evident that the biaxial strength of this material is excellent—essentially 300,000 psi at room temperature and at -105°F. There was a wider spread of burst strength values at -105°F than at 75°F, but there are insufficient data to take this as an indication of a tendency toward "brittleness." However, the fracture-appearance data for the vessels do indicate a possible tendency toward brittleness at -105°F.

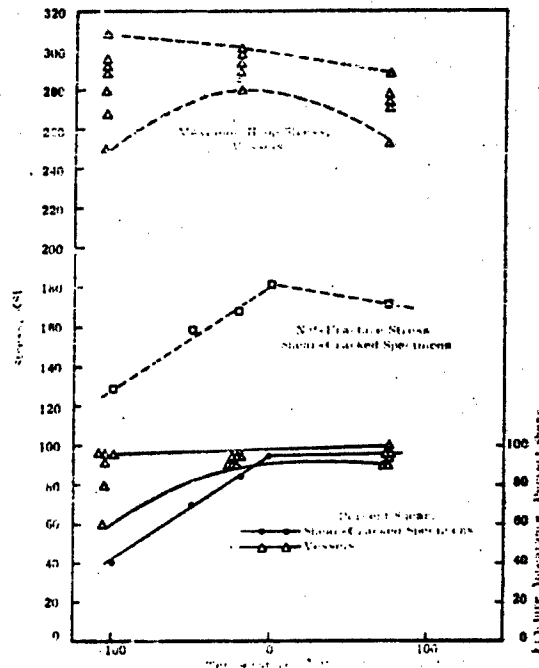


Figure 24 Relationship between the shear properties of AISI 4340 steel, vessels, and the fracture process. The data are for the shear properties of AISI 4340 steel.

<sup>1</sup> Hardened and tempered at 425° F.

Here are shown the results of the evaluation of the AISI 4340 steel (vacuum remelted) vessels and the comparative data obtained with shear-cracked specimens from the same sheet stock as the vessels. Originally, it was planned to evaluate 4340 model vessels heat treated to two nominal strength levels—180,000 psi and 290,000 psi. However, it was found that the vacuum-remelt 4340 sheet stock, from which the vessels were formed, had been decarburized to a considerable degree at some stage in the processing of the sheet. Since the 290,000 psi strength level could not be attained with the decarburized stock, it was decided to use one heat treatment for all of the vessels. The vessels were hardened and then tempered at 425° F, this treatment producing a range of nominal strength from 240,000 psi to 282,000 psi in companion tensile bars

Because of the limited amount of sheet stock available, vessels fabricated from the 4340 stock were of smaller diameter (3.52 in.) than were the 4130 vessels (5.21 in.) described previously and shown in Figure 3. The length of the cylindrical section of the 4340 vessels was approximately 9.5 in., and the nominal wall thickness was 0.095 in. Burst properties of these vessels were determined at three temperatures, 75° F (six vessels), -20° F (six vessels), and -105° F (seven vessels).

As is shown in Figure 24, the highest and most consistent values of biaxial strength were obtained at -20° F. Because of the much wider spread in burst strengths obtained at -105° F, together with the generally lower values at -105° F, it is probable that -20° F can be taken as an approximate "transition temperature" for the vessels. The same trend is reflected in the fracture-appearance data for the vessels. It is interesting that the net-fracture-strength data and the fracture-appearance data obtained with shear-cracked specimens also tend to show a transition from ductile to brittle behavior of this 4340 material in the same general temperature region, specifically at 0° F for the shear-cracked specimens. It should be pointed out that the 20-degree discrepancy between transition temperatures for the vessels and the shear-cracked specimens may be due in part to a thickness difference. The shear-cracked specimens were prepared from a piece of the original sheet stock from which the bottles were formed, this stock being initially 0.120 in. thick. The final thickness of the vessel walls was 0.095 in. It might be expected that the shear-cracked specimens would exhibit a slightly higher transition temperature than the thinner material of the vessel walls (4).

On the basis of these limited data presented in Figure 24 for the AISI 4340 steel, it seems evident that there is, to a significant degree, a correlation between the burst properties of the vessels and the net-fracture-strength data and fracture-appearance data obtained with crack-propagation specimens. These comparative data show that at temperatures below 0° F there is much greater probability of premature failure of the vessels at relatively low applied stresses even though these vessels are relatively free from fabrication defects such as might be present in weld zones. The detrimental effects of such fabrication defects as are sometimes present in welds on the biaxial strength of ultra-high-strength sheet materials has been recently demonstrated by other investigators (9).

Photographs of some typical fractured 4340 steel vessels are shown in Figure 25, (for the experiments at 75° F), Figure 26 (-20° F), and Figure 27 (-105° F). One of the vessels, B-14 (Figure 27) burst in a



Figure 25. Typical vessels of AISI 4340 steel (240,000-262,000 psi nominal strength level) fractured at 75° F.





**Figure 26.** Typical vessels of AISI 4340 steel (240,000-262,000 psi nominal strength level) fractured at  $-20^{\circ}\text{F}$ .



Figure 27. Typical vessels of AISI 4340 steel (240,000-262,000 psi nominal strength level) fractured at  $-105^{\circ}\text{F}$ .

rather "typically" brittle manner at  $-105^{\circ}\text{F}$ , at a hoop stress of 269,000 psi. In this "brittle" failure, circumferential extension of the fracture, just above the center of the vessel, cut the vessel in two. This portion of the fracture was almost completely cleavage (flat tensile), whereas the main longitudinal fracture in this vessel was 60% shear. It is interesting that, at each temperature, the lowest burst strengths were obtained with vessels that exhibited "smooth" fracture surfaces, consisting largely of shear, but with the fracture extending in one plane in one direction from the point of initiation in the wall and in another plane in the other direction from the initiation point. In the vessels with the highest burst strengths, the fracture surfaces on each side of the initiation points tended to alternate from one plane to another, creating a "serrated" effect. These phenomena are evident in the photographs of the vessels, Figures 25-27.

It has been stated that the 4340 sheet stock, from which the bottles were formed, was known to have been decarburized to a significant, but variable, extent. To give added insight into the behavior of the 4340 vessels, a limited metallographic examination of samples of the vessels was made to determine the degree of decarburization near the point of fracture initiation of each vessel. Inclusion counts were also made on these samples. Samples, adjacent to the metallographic samples, were obtained for chemical analyses for phosphorus, sulphur, and residual gases—oxygen, hydrogen, and nitrogen. The results of these examinations and analyses are presented in Appendix B. p. 108.

#### C. Effects of Experimental Variables on Crack-Propagation Characteristics of Sheet Materials

Certain environmental and material variables have been shown to have a controlling effect on the mechanism by which very high strength materials will fail. Some data have been presented on the effects of sheet thickness (4), and some rather extensive investigations have been made of the effects of nominal strength level on crack-propagation characteristics (5). Some very limited data are available showing the influence, or relative lack of influence, of loading rate on crack-propagation properties (4). In very brief summary, it can be stated that generally these investigations have shown that increasing sheet thickness and increasing nominal strength level both tend to increase the probability of brittle fracture. It might be expected that increasing the loading rate would, by dynamic elevation of the yield strength, also

increase the probability of brittle fracture, although apparently little experimental evidence has been obtained to substantiate this latter conjecture.

In this investigation, the effects of these three variables have been touched upon to a very limited degree. In the following sections, use is made of crack-propagation data already reported in Section IV-A to show the effects of two different tempering temperatures and two different sheet thicknesses on the fracture properties of AISI 4130 steel. Some additional data were obtained for 17-7 PH and AM 350 steels at a very fast loading rate, and these data are compared with the slow-loading-rate data from Section IV-A to show the effects of two different loading rates on fracture properties.

#### 1. Effect of Loading Rate on Crack-Propagation Characteristics

The two sheet materials selected for this study were the austenitic or semi-austenitic, precipitation-hardening stainless steels—17-7 PH and AM 350. Since these materials are characteristically rather unstable, it was believed that they might be responsive to changes in strain rate. Two different types of crack-propagation specimens were used in these experiments. For the AM 350 sheet, shear-cracked specimens and fatigue-cracked specimens were used; for the 17-7 PH sheet, fatigue-cracked specimens only were used. The fatigue-cracked specimens were prepared by axially fatigue-loading specimens with sub-size shear-cracks (0.40 in. long) until the cracks had extended to the desired length (about 0.60 in. over-all).

The samples were loaded to failure within 0.1 sec, in the Southern Research Institute rapid tensile machine, within the same general temperature range used previously to obtain the slow-loading rate data. The two nominal loading rates used were rather widely disparate, being about  $1 \times 10^3$  psi/sec and  $2 \times 10^6$  psi/sec.

The properties obtained for these two alloys at the fast loading rate are shown in Tables 34 and 35 for the AM 350 and Table 36 for the 17-7 PH. The comparative slow-loading-rate data, obtained with fatigue-cracked specimens, appear in Table 35A for the AM 350, and in Table 37, for the 17-7 PH. These tables appear in Appendix A. The effects of loading rates are shown graphically in Figures 28, 29, and 30, which follow.

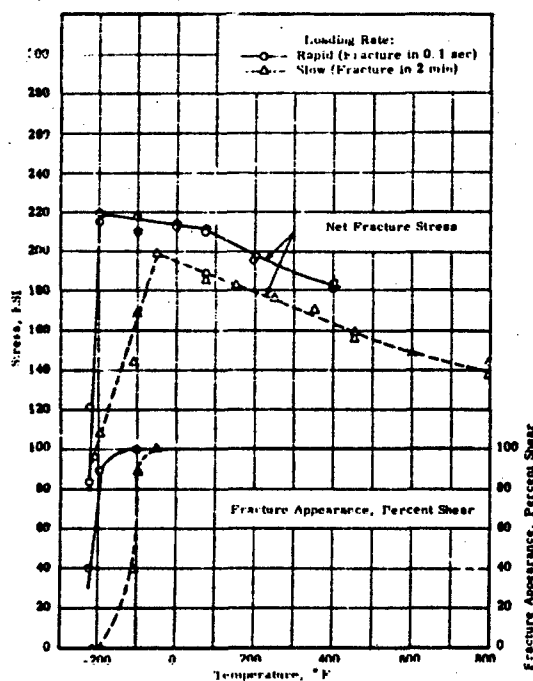


Figure 28 Effect of loading rate on the fracture properties of longitudinal, shear-cracked, AM 350 sheet at various temperatures.

<sup>1</sup> Solution treated at 1725°F 30 min (as-quenched), water quenched; reheat treated at 1050°F 3 hr; aged at 850°F 3 hr.

Figure 28 shows the effect of the two different loading rates on shear-cracked specimens of AM 350 sheet (SCT - 850 condition, 0.040 in. thick). Apparently, greatly increasing the loading rate had the effect of decreasing the brittle-to-ductile transition temperature of this alloy. The effect is evident for both the net fracture stress and the fracture appearance.

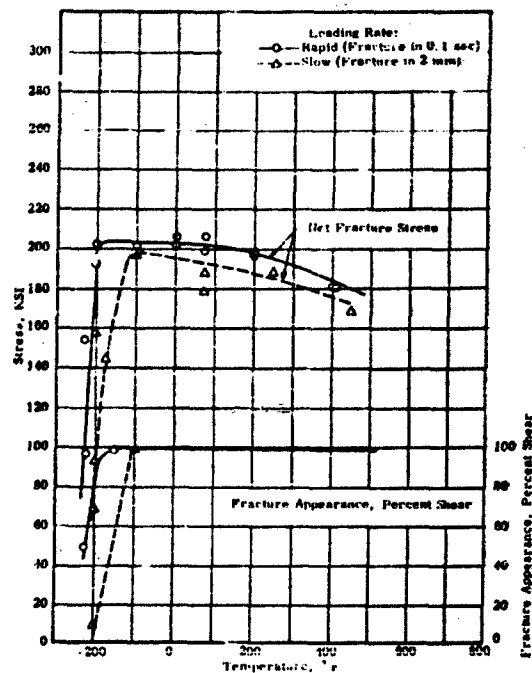


Figure 29. Effect of loading rate on the fracture properties of longitudinal, fatigue-cracked AM 350 sheet<sup>1</sup> at various temperatures.

<sup>1</sup> Solution-treated at 1725°F for 30 min (argon), water-quenched, refrigerated at -105°F 3 hr, aged at 850°F 3 hr.

Figure 29 compares the effects of the two loading rates using fatigue-cracked specimens of the AM 350 sheet (SCT - 850 condition, 0.040 in. thick). Here, generally the same results are shown as in Figure 28, for shear-cracked specimens: a lowering of the transition temperature with increased loading rate.

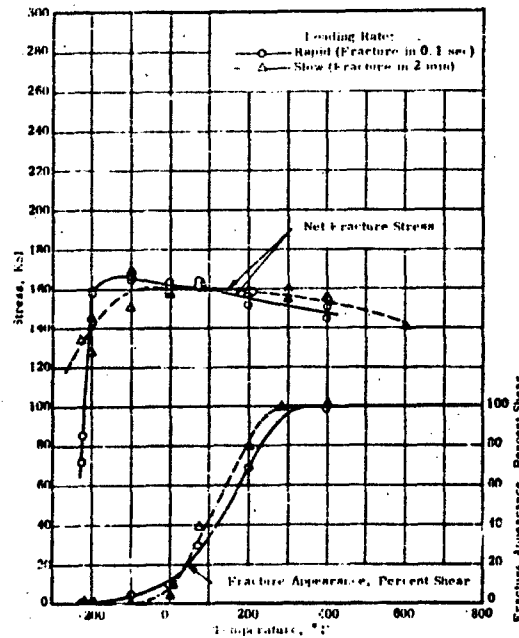


Figure 36 Effect of loading rate on fracture appearance at various temperatures of heat-treated longitudinal fatigue-cracked specimen of 17-7 PH sheet

TH 1050 conditions: 1400°F for 90 min; 50°F for 80 min; 1050°F for 90 min.

The effect of increasing the loading rate for 17-7 PH (TH 1050) sheet was to "sharpen" the net-fracture-stress transition temperature and to increase slightly the fracture-appearance transition temperature.

2. Effect of Tempering Temperature on Transition Temperature of AISI 4130 Steel

It has already been mentioned that considerable data have been obtained showing that heat treatment (nominal strength level) has a pronounced influence on the crack-propagation properties of high-strength sheet alloys. Generally, the higher the nominal strength level, the greater is the notch sensitivity of the material.

There are certain exceptions to this general rule. Srawley and Beachem (6) reported exceptions in the case of a low alloy steel, AMS 6434. Another such exception was evident in this investigation for AISI 4130 steel.



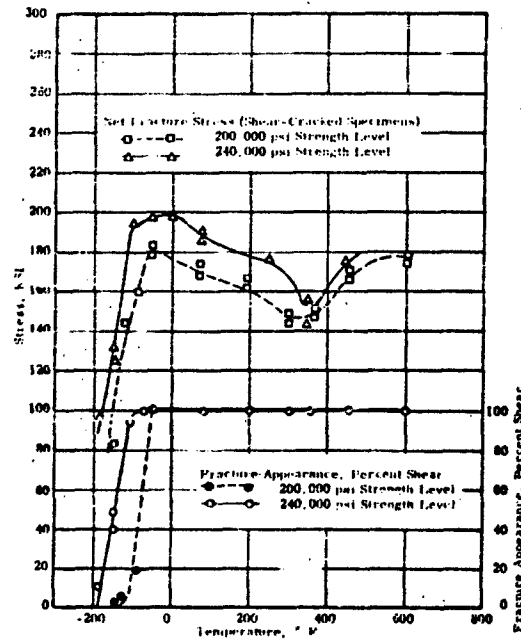


Figure 31 Effect of tempering temperature on the crack-propagation properties of AISI 4130 steel sheet (0.100 in. thick) at various temperatures

The 200,000 psi strength level was produced by tempering at 825° F; the 240,000 psi strength level was produced by tempering at 400° F.

In the above figure, net-fracture stress data and fracture-appearance data, obtained with shear-cracked specimens of 0.100-in.-thick AISI 4130 steel at two strength levels, are plotted as a function of test temperature. The two nominal strength levels were 200,000 psi (obtained by tempering at 825° F) and 240,000 psi (obtained by tempering at 400° F). Here, it is evident that the higher nominal-strength-level material had the lower brittle-ductile transition temperature.

### 3. Effect of Sheet Thickness on Transition Temperature of AISI 4130 Steel

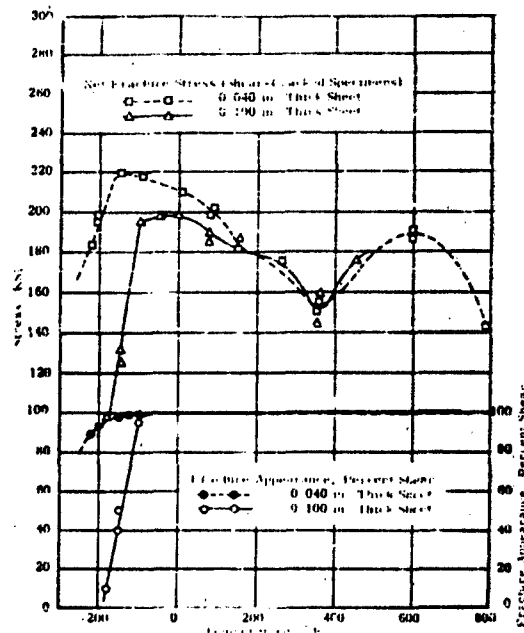


Figure 32 Effect of sheet thickness on the crack-propagation properties of AISI 4130 steel (at the 240,000 psi strength level), at various temperatures.

In Figure 32, the crack-propagation properties of two different thicknesses—0.040 in. and 0.100 in.—of AISI 4130 sheet, at the 240,000 strength level, are compared; shear-cracked specimens were used. As would be expected, the thinner sheet samples showed the lower transition temperature.

#### D. Comparison of Crack-Propagation Data Obtained with Different Types of Specimens

It was one of the purposes of this investigation to attempt to establish the validity of a relatively simple, inexpensive laboratory specimen for assessing the fracture toughness of various high-strength sheet materials. It was felt that the shear-cracked specimen represented an extremely promising design from the standpoints of ease of production and uniformity of notch dimensions. It was then necessary to check its

validity by a direct comparison of data obtained with shear-cracked specimens and with other specimen designs generally accepted as valid.

Some directly comparable data were presented in Section IV, C-1 of this report for shear-cracked specimens and fatigue-cracked specimens of AM 350 sheet fractured at a fast loading rate. This comparison showed that very similar crack-propagation data were obtained with these two types of specimens. In the remainder of this section, additional data, obtained with fatigue-cracked specimens of a number of sheet materials, will be compared with data obtained with shear-cracked specimens of the same materials. The shear-cracked-specimen data were utilized previously in the section on "Evaluation of Crack-Propagation Properties of Sheet Materials."

The materials for which fatigue-cracked specimens were obtained are as follows:

Material	Sheet Thickness, In.	Condition
AM 350	0.040	SCT-850
17-7 PH	0.040	TH 1050
7075 Al	0.064	T-6
7079 Al	0.064	T-6
2024 Al	0.064	T-86
X 2020 Al	0.064	T-6
AISI 4130	0.100	Oil-quenched from 1700° F, tempered at 825° F for 1 hr

The specimens of the thinner sheet materials were fatigue-cracked at Southern Research Institute. The AISI 4130 steel specimens were cracked at the Navy Air Material Center, Philadelphia, through the courtesy of Mr. F. S. Williams.

The crack-propagation data obtained with the fatigue-cracked specimens are shown in tables (Appendix A) and are presented in graphs with the comparable data from shear-cracked specimens. The tables and graphs are identified in the following list:

<u>Sheet Material</u>	<u>Table No.</u>	<u>Figure No.</u>
AM 350	35A	33
17-7 PH	37	34
7075-T6 Al	38	35
7079-T6 Al	39	36
2024-T86 Al	40	37
X 2020-T6 Al	41	38
AISI 4130 (200,000 psi level)	42	39

The figures showing the comparative data for fatigue-cracked and shear-cracked specimens of the above materials appear in the following pages.

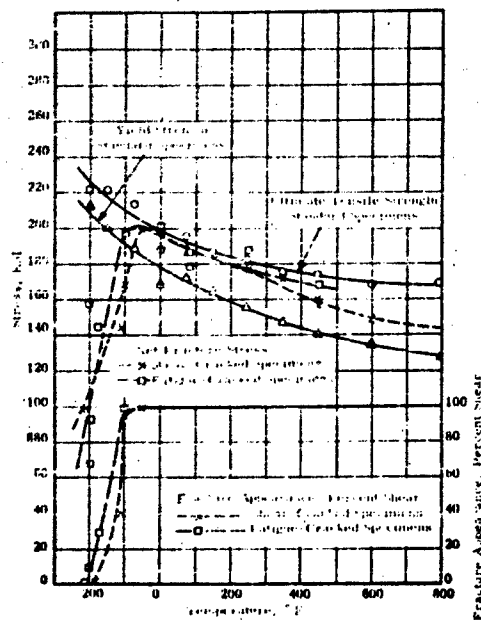


Figure 32. Effect of temperature on the strength of A1.350 sheet. The graph shows the yield strength, ultimate tensile strength, and fatigue strength of A1.350 sheet, loaded to 100% of the yield strength.

The yield strength of 1725 psi at 300°F is shown. A representative fatigue crack growth rate of 105 in./cyc. is shown at 650°F in Figure 33.

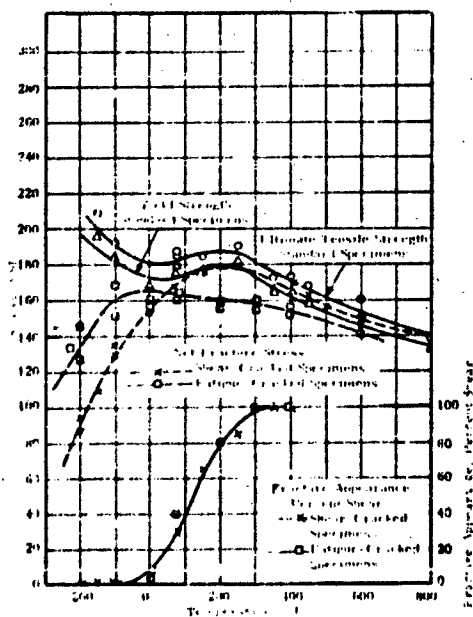


Figure 33. Effect of temperature on the strength of A1.350 sheet. The graph shows the yield strength, ultimate tensile strength, and fatigue strength of A1.350 sheet, loaded to 100% of the yield strength.

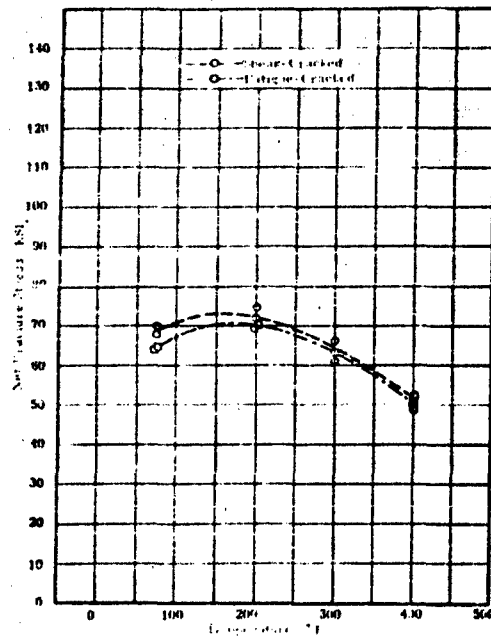


Figure 35. Comparison of the strength characteristics of 7075-T6 aluminum alloy in the as heat treated condition and after 1000 hours at 400°C. The strength characteristics of 7075-T6 aluminum alloy in the as heat treated condition are shown in Figure 34.

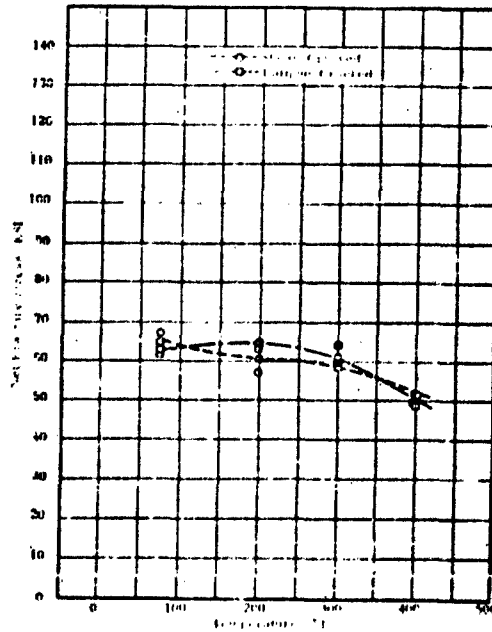


Figure 36. Comparison of the strength characteristics of 7075-T6 aluminum alloy in the as heat treated condition and after 1000 hours at 400°C. The strength characteristics of 7075-T6 aluminum alloy in the as heat treated condition are shown in Figure 34.

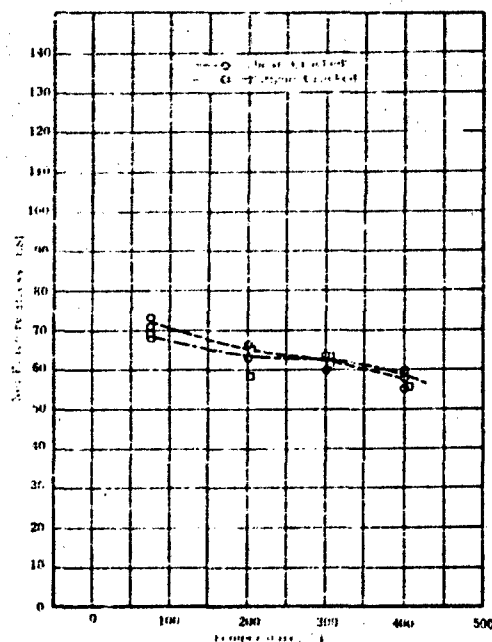


Figure 37. Fatigue crack growth data obtained with stress corrosion and fatigue cracked specimens of 2024-T3 aluminum alloy. Test load of 1000 lbf. Failure at various temperatures after holding for 1000 hr at temperature.

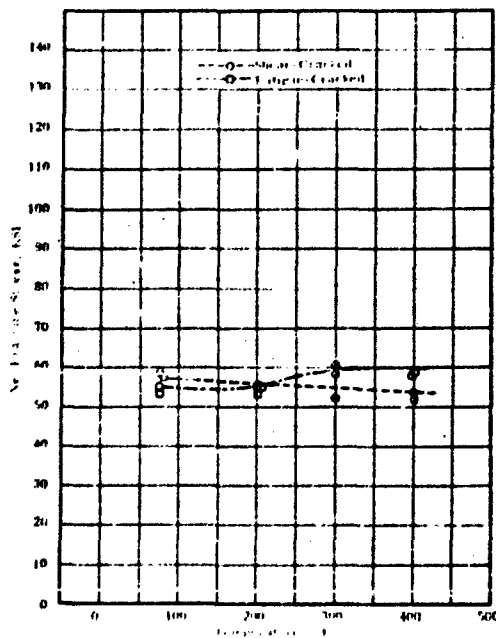


Figure 38. Fatigue crack growth data obtained with stress corrosion and fatigue cracked specimens of 2020-T4 aluminum alloy. Test load of 1000 lbf. Failure at various temperatures after holding for 1000 hr at temperature.

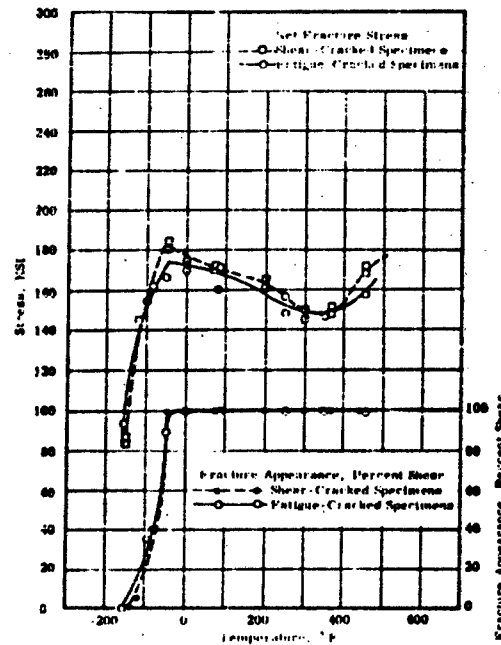


Figure 39 Comparison of fracture properties at various temperatures obtained with two different types of crack propagation specimens of A1574130 steel.

All specimens longitudinal; austempered at 1700° F for 90 min, oil quenched; tempered at 825° F for 1 hr (nominal tensile strength, 200,000 psi).

It is felt that the data presented in the foregoing figures show a good degree of correlation between the shear-cracked and fatigue-cracked specimens for these materials.

It should be noted, at this point, that a comparison of three types of crack-propagation specimens has been undertaken jointly by the NASA Lewis Research Center and the Naval Research Laboratory. The specimen-types are: sharp edge notched (NASA), central fatigue-cracked (NRL), and shear-cracked (SRI). Three materials are being used, all nominally 1/16 in. thick—an H-11 steel, Type 301 stainless steel (70% cold reduced), and an all-beta titanium (B 120 VCA); two specimen widths were chosen—1 in. over-all, and 3 in. over-all. Some of the data obtained in this joint effort have been reported (7, 8) for the H-11 steel.



and the 301 steel. The results of the comparison with the B 120 VCA are not known. In general, this comparison tends to show that the shear-cracked specimen is equivalent in sensitivity to fatigue-cracked specimens of H-11 steel and equivalent to or superior to edge-notched specimens of the H-11. The shear-cracked specimen is less sensitive than the other two types of crack-propagation specimens for the cold-worked 301 steel.

## V. CONCLUSIONS

1. Comparisons made of the crack-propagation characteristics and biaxial strengths of two high-strength sheet materials have indicated that the cracked or notched sheet specimen may be useful for predicting the biaxial strength properties of materials heat treated to very high strength levels (probably greater than 250,000 psi). At strength levels below about 250,000 psi, it seems probable that the properties obtained with the sheet-type crack propagation specimens do not reflect the biaxial strength properties of these materials.

2. Evaluations of four aluminum sheet alloys for aircraft applications, made under highly specialized conditions of heating and loading, have furnished a basis for rating these materials as to their relative resistance to crack-propagation. Of the four alloys evaluated under these conditions, the X 2020 T6 was found to be the most "brittle," the 7079-T6 was found to be the least "brittle," and the 7075-T6 and 2024-T86 were intermediate in properties between the other two alloys.

3. In an investigation of the effect of sheet thickness on the crack-propagation characteristics of AISI 4130 steel, it was found, as expected, that increasing the sheet thickness tended to increase the transition temperature of the material.

4. The effects of two widely different loading rates on the crack-propagation properties of two rather unstable precipitation-hardening alloys—AM 350 and 17-7 PH—were investigated. It was found that a large increase in loading rate apparently may either increase or decrease the transition temperature of this class of materials, depending upon the characteristics of the individual materials.

5. Comparisons made with shear-cracked specimens and fatigue-cracked specimens of seven sheet alloys have shown that generally very similar crack-propagation properties are obtained with these two types of specimens.

BIBLIOGRAPHY

1. "Fracture Testing of High-Strength Sheet Materials. A Report of a Special ASTM Committee." ASTM Bulletin, January 1960, p. 29.
2. J. E. Srawley and C. D. Beachem, "Crack Propagation Tests of High-Strength Sheet Materials, Part III—Low-Alloy Air-Hardening Steel," U. S. Naval Research Laboratory Report 5348, July 30, 1959.
3. J. E. Srawley and C. D. Beachem, "The Effect of Small Surface Cracks on Strength," Prepared Discussion Presented at Seventh Sagamore Conference on Ordnance Materials Research, Raquette Lake, New York, August 16-19, 1960.
4. J. E. Srawley and C. D. Beachem, "Crack Propagation Tests of High-Strength Sheet Steels Using Small Specimens," U. S. Naval Research Laboratory Report 5127, April 9, 1958.
5. G. B. Espey, M. H. Jones, and W. F. Brown, "The Sharp Edge Notch Tensile Strength of Several High-Strength Steel Sheet Alloys," Presented at the Sixty-second Annual Meeting, American Society for Testing Materials, June 21-26, 1959.
6. J. E. Srawley and C. D. Beachem, "Crack Propagation Tests of High-Strength Sheet Materials, Part V—Air-Melted and Consutrode AMS 6434 Steel," U. S. Naval Research Laboratory Report 5507, August 18, 1960.
7. W. F. Brown, Jr. "Mechanical Screening Tests for Sheet Alloys," Presented at Seventh Sagamore Conference on Ordnance Materials Research, Raquette Lake, New York, August 16-19, 1960.
8. A. G. Holms, "NRL-NASA -SRI Cooperative Study of High Strength Sheet Specimens Intended for Measuring Design Values of Crack Toughness," Prepared Discussion Presented at Seventh Sagamore Conference on Ordnance Materials Research, Raquette Lake, New York, August 16-19, 1960.
9. K. E. Caine, J. M. Hodge, R. D. Manning, W. J. Murphy, H. J. Nichols and H. M. Reichhold, "Simulated Service Evaluations of Steels for Solid-Propellant Missile Motor Cases," Technical Report Project No. 40 02-070(2)TD263, Applied Research Laboratory, United States Steel Corporation, Monroeville, Pennsylvania.

APPENDIX A

Data Tables Containing Standard Tensile Properties and  
Crack-Propagation Properties of Sheet Specimens and  
the Burst Properties of Model Pressure Vessels

Table 3

Tensile Properties of Heat-Treated<sup>1</sup> AMS 6434 Steel Sheet<sup>2</sup> at Different Temperatures, and at a Nominal Strain Rate of 0.0001 in. /in. /sec

Specimens Heated to Elevated Test Temperature Within 10 Sec and Held for 10 Sec Before Loading

Temp ° F	0. 2%-Offset Yld Str.	Ultimate Str.	Elong. in 2 in. %
	KSI		
-155	228. 0	269. 0	8. 0
-140	231. 5	274. 5	5. 5
-100	227. 0	268. 0	7. 0
-100	225. 0	270. 0	7. 5
Avg	226. 0	269. 0	7. 3
0	220. 0	261. 0	7. 0
75	203. 0	245. 0	6. 0
75	208. 5	249. 0	6. 0
Avg	205. 3	247. 0	6. 0
150	209. 0	250. 5	7. 0
250	207. 0	252. 5	6. 0
300	214. 0	266. 0	6. 0
350	213. 0	272. 0	6. 0
400	208. 0	255. 0	7. 0
450	179. 0	228. 0	6. 5
450	180. 0	228. 0	7. 0
	179. 5	228. 0	6. 8
600	166. 8	202. 0	7. 5
600	167. 0	208. 5	7. 0
	166. 9	205. 3	7. 3

<sup>1</sup> Austenitized at 1620° F for 30 min (argon), oil quenched; tempered at 400° F for 2 hr.

<sup>2</sup> Longitudinal specimens with gage sections 2 in. long, 3/8 in. wide and 0.064 in. thick.

Table 4

Fracture Strength of Cracked Heat-Treated<sup>1</sup> AMS 6434 Steel Sheet<sup>2</sup>  
at Different Temperatures

Specimens Loaded to Failure at a Free Crosshead-Travel Rate  
of 0.01 in. /min

Temp ° F	Net Fracture Stress, KSI	Fracture Appearance, Percent Shear
-200	80.0	5
-200	94.0	5
Avg	87.0	
-175	119.0	10
-150	134.0	40
-150	119.5	40
Avg	126.8	
-125	211.0	95
-100	212.0	100
0	218.0	100
75	203.0	100
150	207.0	100
250	187.0	100
300	176.0	100
400	172.0	100
500	199.0	100
600	196.0	100

<sup>1</sup> Austenitized at 1620° F for 30 min (argon), oil quenched; tempered  
at 400° F for 2 hr.

<sup>2</sup> Shear-cracked specimens (longitudinal); overall width 1 1/2 in. ;  
thickness 0.064 in. ; crack-length to specimen-width ratio 0.35.

Table 5

Tensile Properties of Heat-Treated<sup>1</sup> 300 M Steel Sheet<sup>2</sup> at Different Temperatures, and at a Nominal Strain Rate of 0.0001 in./in./sec

Specimens Heated to Elevated Test Temperature Within 10 Sec and Held for 10 Sec Before Loading

Temp. ° F	0.2%-Offset Yld. Str.	Ultimate Str.	Elong. in 2 in. %
	KSI		
-150	265.0	283.0	2.0
-100	262.0	287.0	6.0
0	250.0	278.0	3.0
75	257.5	285.0	3.0
150	258.0	295.0	4.5
250	235.5	273.0	4.0
250	234.0	278.0	5.0
Avg	234.8	275.5	4.5
350	239.0	295.0	4.0
400	243.0	286.0	4.5
400	235.0	281.0	3.0
Avg	239.0	233.5	3.8
500	218.5	259.0	7.0
500	213.0	259.5	4.0
500	214.0	270.0	3.0
	215.2	262.8	4.7
600	208.0	242.0	5.0
800	151.0	183.0	5.5

<sup>1</sup> Austenitized at 1600° F for 30 min (argon), oil-quenched; double tempered at 600° F for 3 hr each cycle.

<sup>2</sup> Longitudinal specimens with gage sections 2 in. long, 3/8 in. wide and 0.080 in. thick.

Table 6

Fracture Strength of Cracked Heat-Treated<sup>1</sup> 300 M Steel Sheet<sup>2</sup>  
at Different Temperatures

Specimens Loaded to Failure at a Free Crosshead-Travel Rate  
of 0.01 in. /min

Temp ° F	Net Fracture Stress, KSI	Fracture Appearance, Percent Shear
-200	51.4	0
-80	127.0	45
0	137.5	60
30	142.2	65
75	140.3	78
150	147.3	100
250	132.1	100
350	111.4	100
450	103.0	100
600	113.5	100
800	164.0	100

<sup>1</sup> Austenitized at 1600° F for 30 min (argon), oil quenched; double tempered at 600° F for 3 hr each cycle.

<sup>2</sup> Shear-cracked specimens (longitudinal); overall width 1 1/2 in. ; thickness 0.080 in. ; crack-length to specimen-width ratio 0.35.



Table 7

Fracture Strength of Cracked Full-Hard<sup>1</sup> Type 301 Stainless Steel Sheet<sup>2</sup>  
at Different Temperatures

Specimens Loaded to Failure at a Free Crosshead-Travel Rate  
of 0.01 in./min

Temp ° F	Net Fracture Stress, KSI	Fracture Appearance, Percent Shear
-200	178.0	100
-200	180.5	100
Avg	179.3	100
0	175.0	100
75	174.0	100
75	170.0	100
Avg	172.0	100
150	170.0	100
250	161.0	100
250	154.0	100
Avg	157.5	
350	153.0	100
450	147.0	100
450	146.5	100
Avg	146.8	
600	141.0	100
600	141.0	100
Avg	141.0	

<sup>1</sup> Fifty-percent cold-reduced.

<sup>2</sup> Shear-cracked specimens (longitudinal); overall width 1 1/2 in.; thickness 0.046 in.; crack-length to specimen-width ratio 0.35.

Table 8

Tensile Properties of Heat-Treated<sup>1</sup> AISI 4130 Steel Sheet<sup>2</sup> at  
Different Temperatures, and at a Nominal Strain Rate of  
0.0001 in. /in. /sec

Specimens Heated to Elevated Test Temperature Within 10 Sec  
and Held for 10 Sec Before Loading

Temp ° F	0.2%-Offset Yld. Str.	Ultimate Str.	Elong. in 2 in. %
	ksi		
-200	245.5	268.5	6.0
-150	229.5	253.0	5.5
-100	226.0	247.0	5.5
75	211.0	239.5	4.5
75	210.0	242.0	5.5
	210.5	240.8	5.0
150	206.5	241.5	4.0
150	201.0	241.0	4.0
	203.8	241.3	4.0
250	200.0	242.0	3.0 <sup>3</sup>
300	205.0	247.0	6.5
350	203.5	253.5	3.5 <sup>3</sup>
350	198.0	256.0	4.0 <sup>3</sup>
	200.8	254.8	3.8
400	187.0	241.5	6.5
500	177.0	218.0	6.5
600	158.0	186.0	6.0
800	122.5	131.0	5.0

<sup>1</sup> Austenitized at 1570° F 30 min (argon); oil-quenched; tempered at 400° F for 2 hr.

<sup>2</sup> Longitudinal specimens with gage sections 3/8 in. wide, 2 in. long and 0.042 in. thick.

<sup>3</sup> Specimen fractured at gage point.

SOUTHERN RESEARCH INSTITUTE

Table 9

Fracture Strength of Cracked Heat-Treated<sup>1</sup> AISI 4130 Steel<sup>2</sup>  
at Different Temperatures

Specimens Loaded to Failure at a Free Crosshead-Travel  
Rate of 0.01 in./min

Temp ° F	Net Fracture Stress KSI	Fracture Appearance, Percent Shear
-225	186.5	90
-200	195.5	95
-200	197.0	95
Avg	196.3	
-150	222.5	100
-100	218.0	100
0	212.5	100
75	200.0	100
75	202.0	100
Avg	201.0	
150	183.0	100
250	174.0	100
350	152.0	100
350	155.0	100
Avg	153.5	
450	176.0	100
600	192.5	100
600	189.0	100
Avg	190.8	
800	142.0	100

<sup>1</sup> Austenitized at 1570° F for 30 min (argon); oil quenched; tempered at 400° F for 2 hr.

<sup>2</sup> Longitudinal shear-cracked specimens; overall width 1 1/2 in.; thickness 0.042 in.; crack-length to specimen-width ratio 0.35.

SOUTHERN RESEARCH INSTITUTE

Table 10

Tensile Properties of Heat-Treated<sup>1</sup> AM 350 Stainless Steel Sheet<sup>2</sup>  
at Different Temperatures and at a Nominal Strain Rate of  
0.0001 in./in./sec

Temp ° F	0.2%-Offset Yld. Str.	Ultimate Str.	Elong. in 2 in. %
	KSI		
-200	213.5	222.0	16.5
-150	200.0	222.0	16.5
- 75	188.5	214.0	16.0
0	168.8	188.5	15.5
75	174.0	196.0	12.0
150	162.5	187.5	9.5
250	156.0	183.0	9.0
350	147.8	176.5	8.0
450	140.8	174.5	8.0
600	136.0	168.2	6.5
800	129.0	170.0	8.5

<sup>1</sup> Solution-treated at 1725° F for 30 min (argon), water-quenched;  
refrigerated at -105° F for 3 hr; aged at 850° F for 3 hr.

<sup>2</sup> Longitudinal specimens with gage sections 2 in. long, 3/8 in. wide,  
and 0.040 in. thick.

Table 11

Fracture Strength of Shear-Cracked Heat-Treated<sup>1</sup> AM 350 Sheet<sup>2</sup>  
at Different Temperatures

Specimens Loaded to Failure at a Free Crosshead-Travel  
Rate of 0.01 in./min

Temp ° F	Net Fracture Stress, KSI	Fracture Appearance, Percent Shear
-215	99.0	0
-200	109.0	0
-110	145.0	40
-100	169.0	95
- 50	199.5	100
0	199.0	100
75	190.0	100
75	187.5	100
Avg	188.8	
150	183.5	100
250	176.5	100
350	172.0	100
450	159.5	100
450	158.0	100
Avg	158.8	
600	149.0	100
800	138.0	100
800	145.0	100
Avg	141.5	

<sup>1</sup> Solution treated at 1725° F for 30 min (argon), water-quenched; refrigerated at -105° F for 3 hr; aged at 850° F for 3 hr.

<sup>2</sup> Shear-cracked specimens (longitudinal): over-all width 1 1/2 in.; thickness 0.040 in.; crack-length to specimen-width ratio 0.35.

Table 12

Tensile Properties of Heat-Treated<sup>1</sup> 17-7 PH Stainless Steel Sheet<sup>2</sup>  
at Different Temperatures, and at a Nominal Strain Rate of  
0.0001 in. /in. /sec

Temp ° F	0.2%-Offset Yld. Str. KSI	Ultimate Str.	Elong. in 2 in. %
-150	195.5	208.0	9.0
-100	183.5	190.5	2.5 <sup>3</sup>
0	168.5	179.5	8.5
75	179.0	184.5	8.0
75	175.0	184.2	8.0
Avg	177.0	184.4	8.0
150	177.0	184.0	8.0
250	181.5	189.0	5.0
350	164.8	172.0	4.5
400	165.0	172.5	4.0
500	158.5	167.4	3.5
600	152.2	159.8	3.0
800	132.0	139.5	4.5

<sup>1</sup> TH 1050 condition: 1400° F for 90 min; cooled to 50° F for 60 min; held at 1050° F for 90 min.

<sup>2</sup> Longitudinal specimens with gage sections 3/8 in. wide, 2 in. long, and 0.040 in. thick.

<sup>3</sup> Specimen fractured outside gage section.

Table 13

Fracture Strength of Shear-Cracked 17-7 PH<sup>1</sup> Stainless Steel Sheet<sup>2</sup>  
at Different Temperatures

Specimens Loaded to Failure at a Free Crosshead-Travel  
Rate of 0.01 in./min

Temp ° F	Net Fracture Stress, KSI	Fracture Appearance, Percent Shear
-200	87.5	0
-200	94.8	0
Avg	91.2	0
-150	111.0	0
-100	130.5	0
-100	134.5	0
Avg	132.5	
0	154.0	10
75	166.0	30
75	167.8	30
Avg	166.9	
150	177.0	65
250	177.5	85
350	167.5	100
350	166.5	100
Avg	167.0	
400	170.0	100
450	163.5	100
500	155.5	100
600	146.3	100

Table 13 (Continued)

Fracture Strength of Shear-Cracked 17-7 PH<sup>1</sup> Stainless Steel Sheet<sup>2</sup>  
at Different Temperatures

Specimens Loaded to Failure at a Free Crosshead-Travel  
Rate of 0.01 in. /min

Temp ° F	Net Fracture Stress, KSI	Fracture Appearance. Percent Shear
800	142.0	100
800	142.0	100
Avg	142.0	

<sup>1</sup> TH 1050 condition—1400° F for 90 min; cooled to 50° F for 60 min;  
held at 1050° F for 90 min.

<sup>2</sup> Shear-cracked specimens; over-all width 1 1/2 in.; thickness 0.040  
in.; crack-length to specimen-width ratio 0.35.



Table 14

Tensile Properties of Heat-Treated<sup>1</sup> AISI 4130 Steel Sheet<sup>2</sup>  
at Different Temperatures and at a Nominal Strain Rate of  
0.0001 in. /in. /sec

Temp ° F	0.2%-Offset Yld. Str. KSI	Ultimate Str. KSI	Elong. in 2 in. %
-150	197.5	210.0	5.5
-145	192.5	207.0	2.0
-100	189.8	210.0	5.0
-100	195.0	215.0	4.5
Avg	192.4	212.5	4.8
-50	187.0	209.5	6.5
-50	197.5	204.5	5.5
Avg	192.3	207.0	6.0
75	184.8	203.0	4.5
75	186.0	198.8	4.5
Avg	185.4	200.9	4.5
150	177.3	197.4	4.5
150	183.0	200.5	4.0
Avg	180.2	199.0	4.3
250	163.0	189.8	4.5
250	174.5	194.5	4.0
Avg	168.8	192.2	4.3
350	168.8	194.8	5.0
350	167.8	190.8	5.0
Avg	167.3	192.8	5.0
450	164.5	190.3	7.0
450	161.5	190.3	6.5
Avg	163.0	190.3	6.8

Table 14 (Continued)

Tensile Properties of Heat-Treated<sup>1</sup> AISI 4130 Steel Sheet<sup>2</sup>  
at Different Temperatures and at a Nominal Strain Rate of  
0.0001 in./in./sec

Temp ° F	0.2%-Offset Yld. Str.	Ultimate Str	Elong. in 2 in.
	KSI		%
600	151.0	179.5	11.0
600	145.0	175.0	10.5
Avg	148.0	177.3	10.8

<sup>1</sup> Austenitized at 1700° F for 68 min (neutral atmosphere),  
oil-quenched; tempered at 825° F for 1 hr.

<sup>2</sup> Standard tensile specimens with gage sections 2 in. long,  
0.375 in. wide, and 0.100 in. thick.

Table 15

Fracture Strength of Shear-Cracked Heat-Treated<sup>1</sup> AISI 4130  
Steel Sheet<sup>2</sup> at Different Temperatures

Specimens Loaded to Failure at a Free Crosshead-Travel Rate  
of 0.01 in. /min

Temp ° F	Net Fracture Stress, KSI	Fracture Appearance, Percent Shear	K <sub>c1</sub> KSI $\sqrt{\text{in.}}$	K <sub>c3</sub> KSI $\sqrt{\text{in.}}$
-150	85.5	0	—	83.0
-150	86.0	0	82.5	84.0
Avg	85.8			
-120	145.0	5	—	150.5
-85	162.0	40		181.0
-50	185.0	100	—	—
-50	181.5	100	—	231.0
Avg	183.3			
75	171.5	100	201.0	229.0
75	172.1	100	—	—
Avg	171.8			
200	163.0	100	—	218.0
200	165.5	100	—	—
Avg	164.3			
300	150.0	100	—	—
300	146.3	100	—	—
Avg	148.2			
365	149.5	100	—	193.0
365	150.5	100	—	194.0
Avg	150.0			
450	171.5	100	—	—
450	169.9	100	—	—
Avg	170.7			

Table 15 (Continued)

Fracture Strength of Shear-Cracked Heat-Treated<sup>1</sup> AISI 4130  
Steel Specimens<sup>2</sup> at Different Temperatures

Specimens Loaded to Failure at a Free Crosshead-Travel Rate  
of 0.1 in./in./min.

Temp ° F	Net Fracture Stress, KSI	Fracture Appearance Percent Shear	K <sub>c1</sub> KSI $\sqrt{\text{in.}}$	K <sub>c2</sub> KSI $\sqrt{\text{in.}}$
600	176.3	100	—	—
600	176.5	100	—	—
Avg	176.4			

<sup>1</sup> Austenitized at 1700° F for 68 min, oil-quenched; tempered for  
1 hr at 825° F.

<sup>2</sup> Shear cracked specimens; over-all width 2.65 in., thickness  
0.100 in.; initial crack length 1.00 in.

Table 16

Tensile Properties of Heat-Treated<sup>1</sup> AISI 4130 Steel Sheet<sup>2</sup> at  
Different Temperatures, and at a Nominal Strain Rate of  
0.0001 in./in./sec

Temp ° F	0.2%-Offset	Ultimate	Elong. in 2 in. %
	Yld. Str. ksi		
-140	219.0	247.0	7.0
-50	219.0	257.0	5.5
80	206.0	238.5	6.0
250	229.0	262.0	7.5
350	212.5	246.0	7.0
450	183.0	229.5	6.5

<sup>1</sup> Austenitized at 1700° F for 1 hr (argon), oil-quenched;  
tempered at 400° F for 1 hr.

<sup>2</sup> Longitudinal specimens with gage sections 2 in. long, 3/8  
in. wide and 0.100 in. thick.

Table 17

Fracture Strength of Shear-Cracked<sup>1</sup> AISI 4130 Steel Sheet<sup>2</sup>  
at Different Temperatures

Specimens Loaded to Failure at a Free  
Crosshead- Travel Rate of 0.01 in./min

Temp ° F	Net Fracture Stress, KSI	Fracture Appearance, Percent Shear	Fracture Toughness, $K_{Ic}$ , KSI $\sqrt{\text{in.}}$
-175	96.3	10	98.5
-150	130.5	50	148.0
-150	126.0	40	140.0
Avg	128.3		144.0
-100	194.0	95	255.0
-50	196.5	100	267.0
0	198.5	100	271.0
80	191.5	100	257.0
80	187.0	100	252.0
Avg	189.3		254.5
250	176.5	100	224.0
350	157.5	100	199.5
350	145.8	100	184.5
Avg	151.7		191.5
450	176.5	100	244.0

<sup>1</sup> Longitudinal shear cracked specimens, 2.65 in. over-all width,  
0.100 in. thick, crack-length to specimen-width ratio 0.38.

<sup>2</sup> Austenitized at 1700° F for 1 hr., oil-quenched; tempered at 400° F  
for 1 hr.

Table 16

Tensile Properties of Heat-Treated<sup>1</sup> AISI 4340 Steel Sheet<sup>2</sup> at  
Different Temperatures and at a Nominal Strain Rate of  
0.0001 in./in./sec

Temp °F	0.2%-Offset Yld. Str.	Ultimate Str.	Elong. in 2 in.
	KSI		%
-140	245.0	282.0	6.5
-140	240.5	277.5	7.0
Avg	242.8	279.8	6.8
-50	238.0	277.0	6.5
-50	240.5	282.5	6.5
Avg	239.3	279.8	6.5
80	230.0	279.5	6.0
80	230.5	278.5	6.0
Avg	230.3	279.0	6.0
250	204.0	266.5	4.5
250	200.0	269.0	4.0
Avg	202.0	267.8	4.3
350	214.0	272.0	5.5
350	215.0	273.0	5.5
Avg	214.5	272.5	5.5
450	188.2	249.5	9.0
450	188.2	241.5	8.0
Avg	188.2	245.5	8.5

<sup>1</sup> Austenitized at 1600° F for 30 min (argon), oil-quenched;  
double tempered at 400° F for 2 hr each cycle.

<sup>2</sup> Longitudinal specimens with gage sections 2 in. long, 3/8  
in. wide, and 0.064 in. thick.

Table 19

Fracture Strength of Shear-Cracked<sup>1</sup> AISI 4340 Steel Sheet<sup>2</sup>  
at Different Temperatures

Specimens Loaded to Failure at a Free  
Crosshead-Travel Rate of 0.01 in./min

Temp ° F	Net Fracture Stress, KSI	Fracture Appearance, Percent Shear	Fracture Toughness, $K_{C3}$ , KSI√in.
-200	82.1	0	57.0
-200	76.4	0	—
Avg	79.2		
-100	109.0	30	82.5
-50	150.0	70	120.0
-50	135.5	50	—
Avg	142.8		
0	174.7	95	160.0
80	183.0	100	175.0
80	187.3	100	—
Avg	185.2		
250	175.0	100	162.0
250	172.5	100	—
Avg	173.8		
350	142.0	100	135.0
350	149.5	100	—
Avg	145.8		
500	194.5	100	192.0
500	186.0	100	—
Avg	190.3		

<sup>1</sup> Specimens shear-cracked by usual method; 1.5 in. over-all width, 0.064 in. thick, crack-length to specimen-width ratio 0.33.

<sup>2</sup> Heat-treated as follows: austenitized at 1600° F for 30 min (argon) oil quenched; double tempered at 400° F for 2 hr each cycle.



Table 19A

Fracture Strength of Shear-Cracked<sup>1</sup> AISI 4340 Steel Sheet<sup>2</sup>  
at Different Temperatures

Specimens Loaded to Failure at a Free  
Crosshead-Travel Rate of 0.01 in./min

Temp ° F	Net Fracture Stress, KSI	Fracture Appearance, Percent Shear	Fracture Toughness, $K_{c3}$ , KSI $\sqrt{\text{in.}}$
-200	67.3	0	47.5
-100	106.5	10	76.6
-50	123.5	45	96.0
0	138.6	95	121.0
80	152.5	100	141.0
250	150.0	100	138.0
350	118.6	100	107.5

<sup>1</sup> Specimens shear-cracked and then rolled flat to eliminate protrusions; 1.5 in. over-all width, 0.064 in. thick, crack-length to specimen-width ratio 0.38.

<sup>2</sup> Heat treated as follows: austenitized at 1600° F for 30 min (argon) oil-quenched; double tempered at 400° F for 2 hr each cycle.

Table 20

Tensile Properties of Aged<sup>1</sup> Inconel X Sheet<sup>2</sup> at  
Different Temperatures and at a Nominal Strain Rate of  
0.0001 in./in./sec

Specimens Heated to Elevated Test Temperature Within  
10 Sec and Held 10 Sec Before Loading

Temp ° F	0.2% Offset Yld. Str. KSI	Ultimate Str. KSI	Elong. in 2 in. %
-100	116.5	165.0	23.0 <sup>3</sup>
0	109.5	157.3	27.0
75	116.0	153.0	22.0 <sup>3</sup>
75	118.0	157.0	26.0
Avg	117.0	155.0	—
150	114.0	148.0	25.5
250	109.0	150.8	24.0
350	106.5	148.0	26.5
400	107.5	148.0	26.0
500	105.8	145.5	26.0
600	104.5	144.2	26.0
800	105.8	141.0	26.0
1000	105.8	137.5	25.0

<sup>1</sup> Aged at 1300° F for 20 hr.

<sup>2</sup> Longitudinal specimens with gage sections 3/8 in. wide, 2 in. long and 0.064 in. thick.

<sup>3</sup> Specimen fractured outside gage section

Table 21

Fracture Strength of Shear-Cracked Inconel X<sup>1</sup> Sheet<sup>2</sup>  
at Different Temperatures

Specimens Loaded to Failure at a Free  
Crosshead-Travel Rate of 0.01 in./min

Temp ° F	Net Fracture Stress, KSI	Fracture Appearance, Percent Shear
-200	139.0	100
-200	140.0	100
Avg	139.5	
-150	137.5	100
-100	137.5	100
-100	136.3	100
Avg	136.9	
0	134.0	100
75	131.0	100
75	132.5	100
Avg	131.8	
150	130.0	100
250	127.5	100
350	126.0	100
350	126.0	100
Avg	126.0	
400	126.0	100
500	124.5	100
600	125.0	100
600	122.0	100
Avg	123.5	

Table 21(Continued)

Fracture Strength of Shear-Cracked Inconel X<sup>1</sup> Sheet<sup>2</sup>  
at Different Temperatures

Specimens Loaded to Failure at a Free  
Crosshead Travel Rate of 0.01 in./min

Temp ° F	Net Fracture Stress, KSI	Fracture Appearance, Percent Shear
800	121.0	100
1000	114.0	100
1000	115.0	100
Avg	114.5	

<sup>1</sup> Aged at 1300° F. for 20 hr.

<sup>2</sup> Longitudinal shear-cracked specimens: over-all width 1 1/2 in.; thickness 0.064 in.; crack-length to specimen-width ratio 0.35.

Table 22

Fracture Strength of Shear-Cracked<sup>1</sup> Heat Treated<sup>2</sup> AISI 4340 Steel  
Sheet at Different Temperatures

Specimens Loaded to Failure at a Free  
Crosshead-Travel Rate of 0.01 in./min

Temp ° F	Net Fracture Stress, KSI	Fracture Appearance, Percent Shear	Fracture Toughness, $K_{C3}$ , KSI $\sqrt{\text{in.}}$
-100	129.0	40	108.0
-50	158.5	70	159.0
-20	168.0	85	183.0
0	171.0	95	205.0
75	181.0	95	198.0

<sup>1</sup> Austenitized at 1600° F for 40 min, oil-quenched; tempered at 425° F for 2 hr.

<sup>2</sup> Shear-cracked specimens were 1.87 in. wide, 0.120 in. thick; nominal crack length 0.63 in.

Table 23

Tensile Properties of 7075-T6 Aluminum Alloy Sheet<sup>1</sup> at  
Different Temperatures, Holding Times, and at a Nominal  
Strain Rate of 0.1 in./in./sec

Specimens Heated to Test Temperature Within 5 Sec

Temp °F	Time at Temp Sec	0.2%-Offset		Ultimate	Elong.
		Yld	Str.	Str.	in 2 in. %
75	—	71.2		80.5	10.0
75	—	71.0		79.8	10.5
Avg		71.1		80.2	10.3
200	0	69.0		76.2	10.0
200	0	68.3		75.7	8.0
Avg		68.7		76.0	9.0
200	1800	66.8		76.3	9.0
200	1800	69.1		77.4	9.0
Avg		68.0		76.9	9.0
300	0	60.5		64.5	7.0
300	0	61.1		65.8	7.5
Avg		60.8		65.2	7.3
300	1800	62.0		68.2	7.5
300	1800	67.9		69.1	8.5
Avg		65.0		68.7	8.0
400	0	50.9		52.1	5.5
400	0	51.6		53.8	5.5
Avg		51.3		53.0	5.5
400	1800	45.2		47.5	6.0
400	1800	44.4		47.0	6.0
Avg		44.8		47.3	6.0

<sup>1</sup> Longitudinal specimens; gage section 2 in. long, 3/8 in. wide and 0.063 in. thick.

Table 24

Fracture Strength of Shear-Cracked 7075-T6 Aluminum Alloy  
Sheet<sup>1</sup> at Different Temperatures and Holding Times

Specimens Heated to Temperature Within 5 Sec  
Specimens Loaded to Failure in 0.1 Sec

Temp ° F	Time at Temp. Sec	Net Fracture Stress, KSI	Fracture Toughness, K <sub>IC</sub> , KSI√in.
75	-	63.2	73.0
75	-	70.0	-
Avg	-	69.1	-
200	0	65.2	65.9
200	0	71.0	-
Avg	0	68.6	-
200	1800	74.8	-
200	1800	72.2	-
Avg	1800	73.5	-
300	0	63.4	63.9
300	0	61.8	-
Avg	0	62.6	-
300	1800	61.1	-
300	1800	66.4	-
Avg	1800	63.8	-
400	0	55.5	54.7
400	0	54.9	-
Avg	0	55.2	-
400	1800	51.0	-
400	1800	52.7	-
Avg	1800	51.9	-

<sup>1</sup> Longitudinal specimens; 1.5 in. over-all width, 0.063 in. thick, crack-length to specimen-width ratio 0.38.

Table 25

Tensile Properties of 7079-T6 Aluminum Alloy Sheet<sup>1</sup> at  
Different Temperatures, Holding Times, and at a Nominal  
Strain Rate of 0.1 in./in./sec

Specimens Heated to Test Temperature Within 5 Sec

Temp ° F	Time at Temp Sec	0.2%-Offset		Ultimate Str.	Elong. in 2 in. %
		Yld Str.	KSI		
75	—	54.5		64.4	9.0
75	—	56.0		65.1	7.0
Avg		55.3		64.8	8.0
200	0	63.3		69.7	8.0
200	0	62.9		70.7	10.5
Avg		63.1		70.2	9.3
200	1800	58.9		66.6	9.0
200	1800	63.3		70.2	9.5
Avg		61.1		68.4	9.3
300	0	58.6		63.3	6.5
300	0	60.5		65.6	6.5
Avg		59.6		64.5	6.5
300	1800	55.2		64.5	11.0
300	1800	56.4		64.4	11.0
Avg		55.8		64.5	11.0
400	0	44.6		48.0	6.0
400	0	44.8		47.7	8.5
Avg		44.7		47.9	7.3
400	1800	39.1		41.5	7.0
400	1800	36.2		39.6	7.0
Avg		37.9		40.6	7.0

<sup>1</sup> Longitudinal specimens: gage section 2 in. long, 3/8 in. wide and 0.063-in. thick



Table 26

Fracture Strength of Shear-Cracked 7079-T6 Aluminum Alloy  
Sheet<sup>1</sup> at Different Temperatures and Holding Times

Specimens Heated to Temperature Within 5 Sec  
Specimens Loaded to Failure in 0.1 Sec

Temp ° F	Time at Temp Sec	Net Fracture Stress, KSI	Fracture Toughness, $K_{IC}$ , KSI $\sqrt{in.}$
75	-	67.9	70.1
75	-	65.2	-
Avg		66.6	-
200	0	59.4	60.2
200	0	59.8	-
Avg		59.6	-
200	1800	57.8	-
200	1800	60.6	-
Avg		59.2	-
300	0	60.2	60.5
300	0	57.8	-
Avg		59.0	-
300	1800	61.0	-
300	1800	60.6	-
Avg		60.8	-
400	0	53.6	56.0
400	0	52.9	-
Avg		53.3	-
400	1800	52.8	-
400	1800	52.9	-
Avg		52.9	-

<sup>1</sup> Longitudinal specimens; 1.5 in. over-all width, 0.063 in. thick,  
crack length to specimen-width ratio 0.38.

Table 27

Tensile Properties of 2024-T86 Aluminum Alloy Sheet<sup>1</sup> at  
Different Temperatures, Holding Times, and at a Nominal  
Strain Rate of 0.1 in./in./sec

Specimens Heated to Test Temperature Within 5 Sec

Temp °F	Time at Temp Sec	0.2%-Offset Yld. Str.	Ultimate Str.	Elong. in 2 in. %
		KSI		
75	—	69.5	71.4	5.0
75	—	68.2	75.5	5.0
Avg		68.9	73.5	5.0
200	0	67.4	69.1	4.5
200	0	71.0	72.6	5.0
Avg		69.2	70.9	4.8
200	1800	65.6	67.2	5.0
200	1800	69.5	70.1	5.0
Avg		67.6	68.7	5.0
300	0	64.0	65.3	4.0
300	0	65.0	66.1	4.0
Avg		64.5	65.7	4.0
300	1800	66.1	68.1	5.0
300	1800	65.0	66.6	5.0
Avg		65.6	67.4	5.0
400	0	59.3	59.9	4.5
400	0	57.1	58.5	4.5
Avg		58.2	59.2	4.5
400	1800	52.4	53.4	5.5
400	1800	55.5	56.7	5.5
Avg		54.0	55.1	5.5

<sup>1</sup> Longitudinal specimens; gage section 2 in. long, 3/8 in. wide,  
0.063 in. thick.

Table 28.

Fracture Strength of Shear-Cracked 2024-T86 Aluminum Alloy  
Sheet at Different Temperatures and Holding Times

Specimens Heated to Temperature Within 5 Sec  
Specimens Loaded to Failure in 0.1 Sec

Temp ° F	Time at Temp Sec	Net Fracture Stress, KSI	Fracture Toughness, $K_{cs}$ , KSI√in.
75	--	73.5	80.0
75	--	71.1	--
Avg		72.3	--
200	0	68.0	72.2
200	0	66.8	--
Avg		67.4	--
200	1800	63.5	--
200	1800	66.4	--
Avg		65.0	--
300	0	60.2	62.8
300	0	64.0	--
Avg		62.1	--
300	1800	63.8	--
300	1800	59.0	--
Avg		61.4	--
400	0	58.1	61.0
400	0	55.8	--
Avg		57.0	--
400	1800	58.3	--
400	1800	56.5	--
Avg		57.4	--

<sup>1</sup> Longitudinal specimens; 1.5 in. over all width, 0.063 in. thick, crack-length to specimen-width ratio 0.38.

Table 29

Tensile Properties of X2020-T6 Aluminum Alloy Sheet<sup>1</sup> at  
Different Temperatures, Holding Times, and at a Nominal  
Strain Rate of 0.1 in./in./sec

Specimens Heated to Test Temperature Within 5 Sec

Temp °F	Time at Temp Sec	0.2%-Offset		Ultimate Str.	Elong. in 2 in. %
		Yld	Str.		
		KSI			
75	—	69.5		71.2	4.5
75	—	70.0		71.2	4.5
Avg		69.8		71.2	4.5
200	0	68.1		72.6	5.5
200	0	68.9		72.3	5.5
Avg		68.5		72.5	5.5
200	1800	64.1		67.4	5.0
200	1800	63.3		65.7	4.5
Avg		63.7		66.6	4.8
300	0	62.9		67.6	5.5
300	0	64.8		68.7	6.5
Avg		63.9		68.2	6.0
300	1800	57.8		61.6	5.5
300	1800	58.2		63.4	5.5
Avg		58.0		62.5	5.5
400	0	54.0		55.0	4.0
400	0	55.5		56.5	4.0
Avg		54.8		55.8	4.0
400	1800	50.0		51.8	5.0
400	1800	52.1		54.3	4.0
Avg		51.1		53.1	4.5

<sup>1</sup> Longitudinal specimens; gage section 2 in. long, 3/8 in. wide,  
0.063 in. thick

Table 30

Fracture Strength of Shear-Cracked X2020-T6 Aluminum Alloy  
Sheet<sup>1</sup> at Different Temperatures and Holding Times

Specimens Heated to Temperature Within 5 Sec  
Specimens Loaded to Failure in 0.1 Sec

Temp ° F	Time at Temp Sec	Net Fracture Stress, KSi	Fracture Toughness, K <sub>c3</sub> , KSi√in.
75	—	58.3	57.0
75	—	55.5	—
Avg		56.9	—
200	0	54.4	52.1
200	0	60.0	—
Avg		57.0	—
200	1800	55.0	—
200	1800	55.8	—
Avg		55.4	—
300	0	58.6	56.6
300	0	55.0	—
Avg		55.8	—
300	1800	58.4	—
300	1800	53.0	—
Avg		55.7	—
400	0	48.0	46.0
400	0	48.2	—
Avg		48.1	—
400	1800	51.8	—
400	1800	54.0	—
Avg		52.9	—

<sup>1</sup> Longitudinal specimens; 1.5 in. over-all width, 0.063 in. thick, crack-length to specimen-width ratio 0.38.

Table 31

Burst Properties of AISI 4130<sup>1</sup> Model Vessels<sup>2</sup> Fractured  
at Different Temperatures

Temp ° F	Burst Pressure, psi	Hoop Stress, KSI	Fracture Appearance, Percent Shear
-160	9650	235.0	75
-105	9700	236.0	90
-105	9400	228.0	90
-105	9300	226.0	90
Avg		222.0	
-5	9100	221.5	100
6	9100	221.5	100
75	9600	234.0	100
75	9100	222.0	100
75	8850	215.0	100
Avg		223.7	
200	8950	218.0	100
200	8800	214.0	100
200	8600	209.0	100
Avg		213.0	
365	8500	207.0	100
365	8000	195.0	100
365	9000	219.0	100
Avg		207.0	

<sup>1</sup> Heat treated as follows: austenitized at 1700° F (neutral atmosphere) for 68 min total time, oil-quenched; tempered at 825° F for 1 hr.

<sup>2</sup> Vessels were seamless, 205 cu in. bottles; nominal wall thickness 0.105 in.

Table 32

Burst Properties of AISI 4130<sup>1</sup> Model Vessels<sup>2</sup> Fractured  
at Different Temperatures

Temp ° F	Burst Pressure, psi	Hoop Stress, KSI	Fracture Appearance, Percent Shear
-105	12,100	294.0	75
-105	12,900	315.0	70
-105	12,900	315.0	75
Avg		308.0	
80	12,200	296.0	95
80	12,500	304.0	95
80	12,300	299.0	95
Avg		299.7	

<sup>1</sup> Heat treated as follows: austenitized at 1700° F (neutral atmosphere) for 68 min total time, oil-quenched; tempered at 400° F for 1 hr.

<sup>2</sup> Vessels were seamless, 205 cu. in. bottles; nominal wall thickness 0.105 in.

Table 33

Burst Properties of AISI 4340<sup>1</sup> Model Vessels<sup>2</sup> Fractured  
at Different Temperatures

Vessel No.	Temp ° F	Burst Pressure, psi	Hoop Stress, KSI	Fracture Appearance, Percent Shear
A-6	-105	15,300	292.5	95
B-14	-105	14,500	269.0	60
A-3	-105	15,800	308.5	95
A-10	-105	15,300	295.5	95
B-4	-105	14,600	251.5	80
A-4	-105	16,000	294.4	95
B-12	-105	14,500	280.0	95
A-7	-20	15,800	299.0	95
A-2	-20	15,900	301.0	90
A-8	-20	15,000	280.0	90
B-8	20	15,800	287.0	95
B-3	-20	15,600	294.5	95
B-9	-20	15,300	289.5	90
B-16	75	13,700	253.8	95
A-9	75	14,700	273.5	90
A-1	75	15,400	289.0	95
B-7	75	14,400	272.0	95
A-5	75	15,000	278.0	100
B-1	75	14,600	276.5	90

<sup>1</sup> Oil quenched from 1600° F; tempered at 425° F.

<sup>2</sup> Vessels were seamless, 3.52 in. in diameter, cylindrical section 9.5 in. long; wall thickness nominally 0.095 in. (varying from about 0.088 in. to 0.102 in.).



Table 34

Fracture Strength of Shear Cracked AM 350<sup>1</sup> Stainless Steel Sheet<sup>2</sup>  
at Different Temperatures

Specimens Loaded to Failure at a Rapid Rate to Produce  
Fracture in 0.1 Sec

Temp ° F	Net Fracture Stress, KSI	Fracture Appearance, Percent Shear
-225	122.0	40
-225	84.3	40
Avg	103.2	
-200	220.5	90
-200	216.0	90
Avg	218.3	
-100	211.5	100
-100	218.5	100
Avg	215.0	
0	214.5	100
0	213.0	100
Avg	213.8	
75	213.0	100
75	211.5	100
Avg	212.3	
200	195.5	100
200	197.0	100
Avg	196.8	
400	181.5	100
400	184.0	100
Avg	182.8	

<sup>1</sup> Solution treated at 1725° F for 30 min (argon), water-quenched;  
refrigerated at -105° F for 3 hr; aged at 850° F for 3 hr.

<sup>2</sup> Shear-cracked specimens (longitudinal); over-all width 1 1/2 in.;  
thickness 0.040 in.; crack-length to specimen-width ratio 0.35.

Table 35

Fracture Strength of Fatigue-Cracked AM 350<sup>1</sup> Stainless Steel Sheet<sup>2</sup>  
at Different Temperatures

Specimens Loaded to Failure at a Rapid Rate to Produce  
Fracture in 0.1 Sec

Temp ° F	Net Fracture Stress, KSI	Fracture Appearance, Percent Shear
-225	155.0	50
-225	96.8	45
Avg	125.9	
-200	202.5	95
-200	192.0	90
Avg	197.3	
-100	201.5	100
0	202.0	100
0	205.0	100
Avg	203.5	
75	205.5	100
75	198.5	100
Avg	202.0	
200	197.0	100
200	198.0	100
Avg	197.5	
400	182.0	100
400	182.0	100
Avg	182.0	

<sup>1</sup> Solution treated at 1725° F for 30 min (argon), water-quenched;  
refrigerated at -105° F for 3 hr; aged at 850° F for 3 hr.

<sup>2</sup> Fatigue-cracked specimens (longitudinal); over-all width 1 1/2 in.;  
thickness 0.040 in.; crack-length to specimen-width ratio 0.35.

Table 35A

Fracture Strength of Fatigue-Cracked Heat-Treated<sup>1</sup> AM 350 Sheet<sup>2</sup>  
at Different Temperatures

Specimens Loaded to Failure at a Free Crosshead-Travel  
Rate of 0.01 in./min.

Temp ° F	Net Fracture Stress, KSI	Fracture Appearance, Percent Shear
-200	93.5	10
-200	158.5	10
-200	69.0	0
Avg	107.0	
-175	145.0	30
100	197.0	100
0	201.0	100
75	188.0	100
75	179.0	100
Avg	183.5	
250	188.0	100
450	169.0	100

<sup>1</sup> Solution treated at 1725° F for 30 min (argon), water-quenched; refrigerated at -105° F for 3 hr; aged at 850° F for 3 hr.

<sup>2</sup> Fatigue-cracked specimens (longitudinal); over-all width 1 1/2 in.; thickness 0.040 in.; crack-length to specimen-width ratio 0.35.

Table 36

Fracture Strength of Fatigue-Cracked 17-7 PH<sup>1</sup> Stainless Steel Sheet<sup>2</sup> at Different Temperatures

Specimens Loaded to Failure at a Rapid Rate to Produce Fracture in 0.1 Sec

Temp ° F	Net Fracture Stress, KSI	Fracture Appearance, Percent Shear
-225	85.3	0
-225	71.8	0
Avg	78.6	
-200	158.8	0
-200	157.5	0
Avg	158.2	
-100	165.7	5
-100	166.4	5
Avg	166.1	
0	161.8	10
0	163.3	10
Avg	162.5	
75	164.2	30
75	161.5	30
Avg	162.9	
200	158.0	60
200	151.0	60
Avg	154.5	
400	145.5	100
400	151.0	100
Avg	148.3	

<sup>1</sup> TH 1050 condition—1400° F for 90 min; cooled to 50° F for 60 min; held at 1050° F for 90 min.

<sup>2</sup> Longitudinal fatigue-cracked specimens; over-all width 1 1/2 in.; thickness 0.040 in.; crack-length to specimen-width ratio 0.35.

Table 37

Fracture Strength of Fatigue-Cracked 17-7 PH<sup>1</sup> Stainless Steel  
Sheet<sup>2</sup> at Different Temperatures

Specimens Loaded to Failure at a Free Crosshead-Travel  
Rate of 0.01 in./min.

Temp ° F	Net Fracture Stress, KSI	Fracture Appearance, Percent Shear
-225	134.0	0
-200	128.0	0
-200	146.0	0
Avg	137.0	
-100	169.0	0
-100	151.0	0
Avg	160.0	
0	158.0	5
0	159.0	10
Avg	158.5	
75	161.0	40
75	164.5	40
Avg	162.8	
200	158.5	80
200	157.0	80
Avg	157.8	
300	154.5	100
300	160.0	100
Avg	157.3	
400	155.0	100
400	154.0	100
Avg	154.5	
600	141.0	100

<sup>1</sup> TH 1050 condition—1400° F for 90 min; cooled to 50° F for 60 min;  
held at 1050° F for 90 min.

<sup>2</sup> Longitudinal fatigue-cracked specimens; over-all width 1 1/2 in.;  
thickness 0.040 in.; crack-length to specimen-width ratio 0.35.

Table 38

Fracture Strength of Fatigue-Cracked 7075-T6 Aluminum Alloy  
Sheet<sup>1</sup> at Different Temperatures

Specimens Held at Temperature for 1800 Sec Before Loading  
Specimens Loaded to Failure in 0.1 Sec

Temp ° F	Net Fracture Stress, KSI
75	64.7
75	64.0
Avg	64.4
200	70.1
200	70.0
Avg	70.1
300	60.0
300	63.4
Avg	61.7
400	48.6
400	50.2
Avg	49.4

<sup>1</sup> Longitudinal specimens; 1.5 in. over-all width; 0.063 in. thick,  
crack-length to specimen-width ratio 0.35 to 0.40.

Table 39

Fracture Strength of Fatigue-Cracked 7079-T6 Aluminum Alloy  
Sheet<sup>1</sup> at Different Temperatures

Specimens Held at Temperature for 1800 Sec Before Loading  
Specimens Loaded to Failure in 0.1 Sec

Temp ° F	Net Fracture Stress, KSI
75	64.3
75	61.6
Avg	63.0
200	65.0
200	63.5
Avg	64.3
300	64.4
300	59.4
Avg	61.9
400	50.5
400	49.2
Avg	49.9

<sup>1</sup> Longitudinal specimens; 1.5 in. over-all width, 0.063 in. thick, crack-length to specimen-width ratio 0.35 to 0.40.

Table 40

**Fracture Strength of Fatigue-Cracked 2024-T86 Aluminum Alloy  
Sheet<sup>1</sup> at Different Temperatures**

**Specimens Held at Temperature for 1800 Sec Before Loading  
Specimens Loaded to Failure in 0.1 Sec**

<u>Temp ° F</u>	<u>Net Fracture Stress, KSI</u>
75	68.3
75	69.1
Avg	68.4
200	65.9
200	58.6
Avg	62.3
300	64.0
300	61.6
Avg	62.8
400	60.0
400	56.3
Avg	58.2

---

<sup>1</sup> Longitudinal specimens, 1.5 in. over-all width, 0.063 in. thick,  
crack-length to specimen-width ratio 0.35 to 0.40.



Table 41

Fracture Strength of Fatigue-Cracked X2020-T6 Aluminum Alloy  
Sheet<sup>1</sup> at Different Temperatures

Specimens Held at Temperature for 1800 Sec Before Loading  
Specimens Loaded to Failure in 0.1 Sec

Temp °F	Net Fracture Stress, KSI
75	53.6
75	58.0
Avg	55.8
200	53.8
200	55.1
Avg	54.5
300	—
300	61.5
Avg	61.5
400	58.0
400	59.8
Avg	58.9

<sup>1</sup> Longitudinal specimens; 1.5 in. over-all width, 0.063 in. thick,  
crack-length to specimen-width ratio 0.35 to 0.40

Table 42

Fracture Strength of Fatigue-Cracked<sup>1</sup> AISI 4130 Steel Sheet<sup>2</sup>  
at Different Temperatures

Specimens Loaded to Failure at a Free  
Crosshead-Travel Rate of 0.01 in./min

Temp ° F	Net Fracture Stress, KSI	Fracture Appearance, Percent Shear
-155	93.6	0
-100	155.0	35
-50	163.5	90
0	170.0	100
0	174.8	100
Avg	172.4	
80	160.5	100
80	172.5	100
Avg	166.5	
250	156.5	100
250	148.8	100
Avg	152.7	
350	146.5	100
450	157.5	100

<sup>1</sup> Longitudinal specimens with shear-cracks initially 0.6 in. long, extended by axial fatigue loading. Over-all specimen width 2.65 in., over all crack lengths from 0.90 in. to 1.00 in.

<sup>2</sup> Austenitized at 1700° F for 68 min, oil-quenched; tempered at 825° F for 1 hr, (nominal tensile strength, 200,000 psi).

APPENDIX B

Chemical Analyses, Depth of Decarburization Measurements,  
and Inclusion Counts on Samples from AISI 4340 Steel Vessels

It is not within the scope of this program to present an exhaustive investigation of the microstructure of the AISI 4340 steel pressure vessels used in the correlative studies. However, it is quite likely that the burst properties of these vessels were to some extent affected by surface decarburization known to be present in the sheet stock from which the vessels were formed. Therefore, depth of decarburization measurements were made on a sample from each vessel. And to give some added insight into the burst behavior of these vessels, it was thought desirable to have chemical analyses made on a few vessel samples for phosphorus, sulfur, nitrogen, oxygen, and hydrogen so that the range of content of these elements in the vacuum-remelted stock could be established. The results of the chemical analyses on four vessels, and depth of decarburization measurements and inclusion counts, made on samples taken near the fracture initiation sites in all of the vessels, are presented in tabular form in this Appendix. The burst properties of the vessels are also given again in these tables so that a direct comparison with decarburization depth can be made. Samples for the decarburization examinations, cut from the fracture initiation area, were about 3/4 in. square and were mounted and polished for microhardness measurements. A microhardness traverse was made across the thickness of each sample about 1/2 in. from the fracture surface. Samples for chemical analyses were taken at a location adjacent to the metallographic samples.

Chemical Analyses on Vessels

<u>Vessel</u>	<u>%P</u>	<u>%S</u>	<u>N</u>	<u>O</u>	<u>H</u>
				<u>ppm</u>	
A-5	<0.01	0.007	106	40	3.7
A-6	<0.01	0.007	116	35	2.2
B-14	<0.01	0.007	123	25	3.3
B-16	<0.01	0.006	129	65	2.3

Decarburization Depth and Inclusion Counts  
on Samples Taken Near Fracture-Initiation Sites

Vessel	Decarburization Depth, in. (Microhardness Traverses)		ASTM Inclusion Rating <sup>1</sup>	Fracture Appearance, % Shear	Hoop Stress at Burst, psi	Evaluation Temperature, ° F
	Inner Wall Surface	Outer Wall Surface				
A-6	0.0032	0.0010	D-1-T	95	292,500	-105
B-14	0.0140	0.0040	D-1-H	60	269,000	-105
A-3	0.0150	0.0152	D-1-H	95	308,500	-105
A-10	0.0140	0.0032	D-1-H	95	295,500	-105
B-4	0.0100	0.0030	D-2-T	80	251,500	-105
A-4	0.0220	0.0040	D-1-T	95	294,000	-105
B-12	0.0020	0.0010	D-1-H	95	280,000	-105
A-7	0.0300	0.0132	D-1-H	95	299,000	-20
A-2	0.0132	0.0040	D-1-H	90	301,000	-20
A-8	0.0130	0.0048	D-2-H	90	280,000	-20
B-8	0.0240	0.0040	D-1-H	95	287,000	-20
B-3	0.0132	0.0070	D-2-H	95	294,000	-20
B-9	0.0020	0.0040	D-1-H	90	289,000	-20
B-16	0.0040	0.0030	D-3-H	95	253,800	75
A-9	0.0040	0.0196	D-1-H	90	273,500	75
A-1	0.0024	0.0032	A-1-H & D-1-H	95	289,000	75
B-7	0.0024	0.0040	A-1-H & D-2-H	95	272,000	75
A-5	0.0224	0.0088	D-2-H	100	278,000	75
B-1	0.0100	0.0050	D-1-H	90	276,000	75

<sup>1</sup> ASTM Designation: E 45-51; method "A", worst field.

It seems probable from the foregoing data that a correlation can be made between depth of decarburization and strength of the vessels. However, it can be pointed out that in the vessels with the lowest burst strengths (B-14, B-4, and B-16), the decarburization was slight to moderate, not exceeding 0.0146 in. and in all three vessels the depth of decarburization did not exceed 0.0040 in.

It is interesting to note that, in the samples for metallographic analyses were made, the inclusion counts are consistent with the oxygen contents. For example, vessel B-16, which had the highest oxygen content, also had the highest oxide-inclusion rating; vessel B-4, which had the lowest oxygen content, had the lowest oxide-inclusion rating.